AD-A034 459 BELL HELICOPTER TEXTRON FORT WORTH TEX F/G 1/3
ROTOR BLADE FLAPPING CRITERIA INVESTIGATION.(U)
DEC 76 L W DOOLEY
UNCLASSIFIED 699-099-021 USAAMRDL-TR-76-33 DAAJ02-75-C-0030 NL

1 OF 2
ADA034459

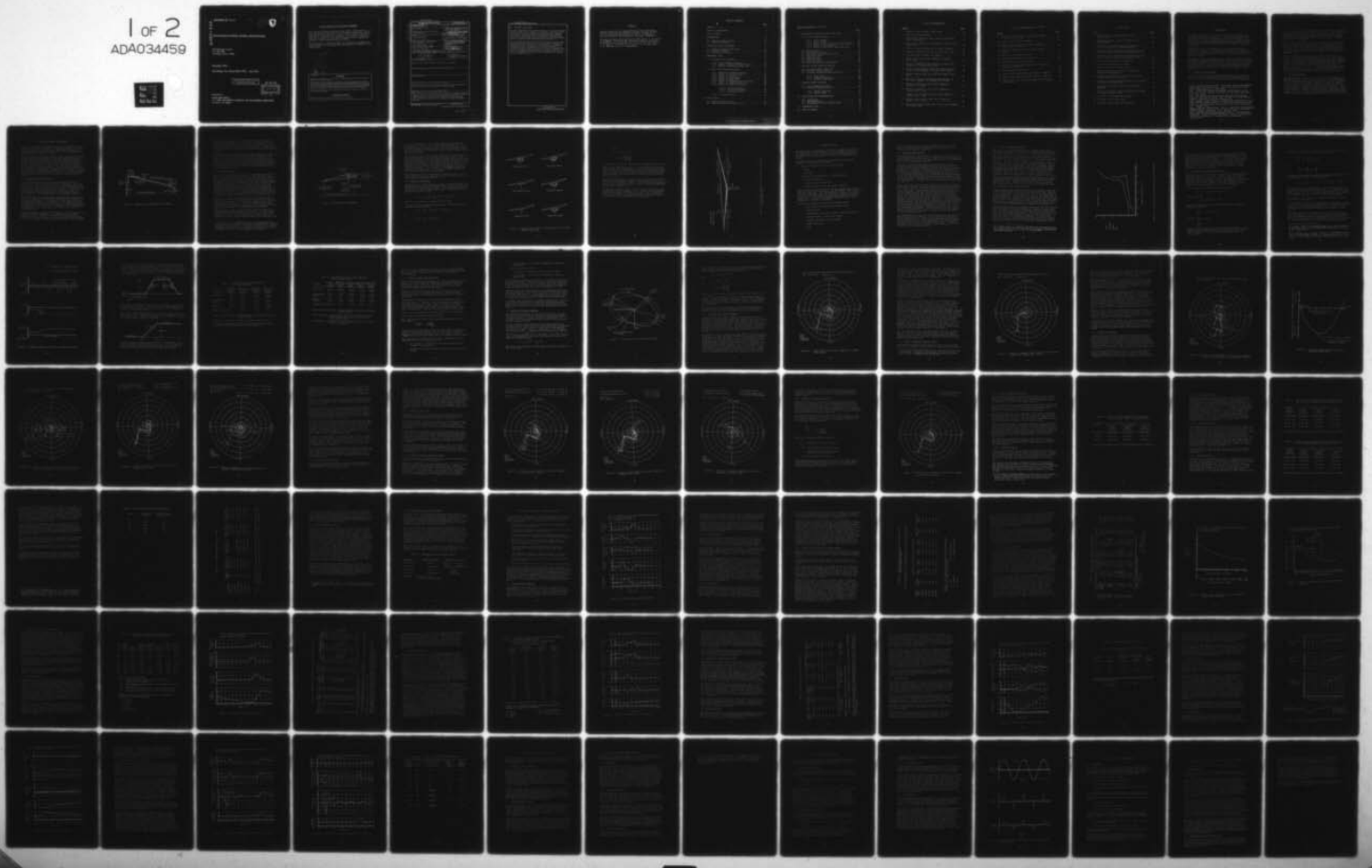

USAAMRDL-TR -76-33

ROTOR BLADE FLAPPING CRITERIA INVESTIGATION

Bell Helicopter Textron
P. O. Box 482
Fort Worth, Texas 76101

December 1976

Final Report for Period April 1975 - July 1976

Prepared for

EUSTIS DIRECTORATE
U. S. ARMY AIR MOBILITY RESEARCH AND DEVELOPMENT LABORATORY
Fort Eustis, Va. 23604

EUSTIS DIRECTORATE POSITION STATEMENT

This report has been reviewed by the Eustis Directorate, U. S. Army Air Mobility Research and Development Laboratory, and is considered to be technically sound. The purpose of this program was to identify rotor parameters and flight conditions that are critical to rotor blade flapping and to attempt to develop a rotor flapping design criteria.

This program was conducted under the technical management of Paul H. Mirick of the Technology Applications Division of this Directorate.

UNCLASSIFIED

SECURITY CLASSIFICATION OF THIS PAGE (When Data Entered)

REPORT DOCUMENTATION PAGE

READ INSTRUCTIONS BEFORE COMPLETING FORM

1. REPORT NUMBER: USAAMRDL-TR-76-33	2. GOVT ACCESSION NO.
3. RECIPIENT'S CATALOG NUMBER	
4. TITLE (and Subtitle): ROTOR BLADE FLAPPING CRITERIA INVESTIGATION.	5. TYPE OF REPORT & PERIOD COVERED: FINAL REPORT. April 1975-July 1976.
6. PERFORMING ORG. REPORT NUMBER: 699-099-021	
7. AUTHOR(s): Larry W. Dooley	8. CONTRACT OR GRANT NUMBER(s): DAAJ02-75-C-0030 NEW
9. PERFORMING ORGANIZATION NAME AND ADDRESS: Bell Helicopter Textron, P. O. Box 482, Fort Worth, Texas 76101	10. PROGRAM ELEMENT, PROJECT, TASK AREA & WORK UNIT NUMBERS: 62209A 1F262209AH76 00 061 EK
11. CONTROLLING OFFICE NAME AND ADDRESS: Eustis Directorate, U.S. Army Air Mobility R&D Laboratory, Fort Eustis, Virginia 23604	12. REPORT DATE: December 1976
	13. NUMBER OF PAGES: 99
14. MONITORING AGENCY NAME & ADDRESS (if different from Controlling Office) 12 100 p.	15. SECURITY CLASS. (of this report): Unclassified
	15a. DECLASSIFICATION/DOWNGRADING SCHEDULE

16. DISTRIBUTION STATEMENT (of this Report)

Approved for public release; distribution unlimited.

17. DISTRIBUTION STATEMENT (of the abstract entered in Block 20, if different from Report)

18. SUPPLEMENTARY NOTES

19. KEY WORDS (Continue on reverse side if necessary and identify by block number)

Rotor flapping, Design criteria, Rotorcraft flight simulation, Flapping in maneuvers, Parametric flapping study

20. ABSTRACT (Continue on reverse side if necessary and identify by block number)

The objective of this study was to identify helicopter characteristics critical to main rotor flapping and to attempt to establish flapping design criteria. Three helicopter types and three rotor systems were simulated in steady flight and maneuvers using the hybrid version of C81, Rotorcraft Flight Simulation Program.

DD FORM 1 JAN 73 1473 EDITION OF 1 NOV 65 IS OBSOLETE

UNCLASSIFIED

SECURITY CLASSIFICATION OF THIS PAGE (When Data Entered)

next page

054200

2B

20. ABSTRACT (Continued)

Critical operational characteristics were: at center of gravity extremes, under low or negative g conditions, with large abrupt control inputs, and in conditions of significant retreating blade stall. Operation outside recommended flight envelopes can cause excessive flapping. Helicopter characteristics influencing flapping were: flapping restraint, fuselage stability characteristics, and helicopter loading conditions.

A limit flapping criterion is defined the same as current design specifications and should apply for all operations within the recommended flight envelopes of the helicopter. An ultimate flapping criterion is proposed for operations outside the recommended flight envelopes and for failure conditions. The ultimate flapping criterion requires no failure of primary structure due to flapping stop contact, and no rotor blade contact with the fuselage for conditions where probability of occurrence is not extremely remote.

PREFACE

The work reported here was performed by Bell Helicopter Textron under Contract DAAJ02-75-C-0030, awarded in April 1975 by the Eustis Directorate of the U. S. Army Air Mobility Research and Development Laboratory (USAAMRDL).

Technical program direction was provided by Mr. P. H. Mirick of USAAMRDL. Principal Bell Helicopter Textron personnel associated with the program were J. M. Davis, L. W. Dooley, H. K. Harr, J. H. Harse, W. A. Kuipers, J. M. Robertson, F. M. Schramm, and J. R. VanGaasbeek.

TABLE OF CONTENTS

		Page
	PREFACE	3
	LIST OF ILLUSTRATIONS	7
	LIST OF TABLES	9
1.	INTRODUCTION	10
	1.1 Current Design Criteria	10
	1.2 Technical Approach	11
2.	SIMULATION MODEL DEVELOPMENT	12
	2.1 General Flapping Description	12
	2.2 Simulation Models	14
	2.3 Flapping Description	16
3.	PARAMETRIC STUDY	20
	3.1 Isolated Rotor Analysis	21
	3.1.1 Rotor Simulation Results	22
	3.1.2 Control Inputs and Angular Rates	24
	3.1.3 Effect of Operating Conditions	30
	3.2 Rotor and Fuselage Combined	31
	3.2.1 Baseline Helicopter Flapping	33
	3.2.2 Center of Gravity Effect	35
	3.2.3 Effect of Sideslip	37
	3.2.4 Effect of Gross Weight	43
	3.2.5 Effect of Rotor RPM	44
	3.2.6 Effect of Fuselage Angle of Attack	44
	3.2.7 Effect of Flapping Restraint	48
	3.2.8 Effect of Blade Flexibility	50
	3.2.8.1 Teetering Rotors	50
	3.2.8.2 Articulated Rotors	52
	3.2.8.3 Hingeless Rotors	52
	3.2.9 Gust Penetration	52
4.	PILOT LIMITS	57
	4.1 Control Movement Limits	57
	4.2 Fuselage Rate and Attitude Limits	58

TABLE OF CONTENTS (Continued)

		Page
5.	SIMULATION OF CRITICAL FLIGHT CONDITIONS	59
	5.1 Roller Coaster Maneuver	59
	5.1.1 High-g Segment	61
	5.1.2 Low-g Segment	61
	5.1.3 Effect of cg Location and Gross Weight	62
	5.1.4 Effect of Hub Restraint	64
	5.1.5 Effect of Helicopter and Rotor Type	68
	5.2 Roll Reversals	68
	5.3 Autorotation Entries	72
	5.4 High Hover Autorotational Entry	75
	5.5 Tail Rotor Loss	75
	5.6 Power-On Flare	77
	5.7 Power-Off Flare	80
	5.8 Hovering Pop-Up	80
	5.9 Hard Landings and Jump Takeoffs	83
6.	CRITICAL FLIGHT CONDITION RESULTS	87
	6.1 Critical Flight Conditions	87
	6.2 Critical Control Inputs	87
	6.3 Critical Helicopter Characteristics	88
	6.3.1 Rotor Type	88
	6.3.2 Fuselage Stability	88
	6.3.3 Loading Conditions	88
7.	FLAPPING DESIGN CRITERIA	90
	7.1 Limit Flapping Criteria	90
	7.2 Ultimate Flapping Criteria	90
	7.2.1 Design Conditions	91
	7.2.2 Design Loads	91
8.	CONCLUSIONS AND RECOMMENDATIONS	93
	8.1 Conclusions	93
	8.2 Recommendations	94
	8.3 Recommendations for Further Study	94
9.	LITERATURE CITED	96
10.	LIST OF SYMBOLS	98

LIST OF ILLUSTRATIONS

Figure		Page
1	Spanwise view of elastic rotor blade	13
2	Rotor blade displacement	15
3	Mathematical models of blade quarter chord lines used in hybrid C81	17
4	Shaft axis flapping for longitudinal flapping and coning only	19
5	Effect of thrust coefficient on rotor flapping	23
6	Flapping response to aft cyclic pitch step input	26
7	Tip path plane in shaft axis system	32
8	Polar plot of main rotor flapping in trimmed level flight	34
9	Effect of sideward flight velocity on main rotor flapping in trimmed level flight	36
10	Effect of longitudinal center of gravity position on main rotor flapping in trimmed level flight	38
11	Elevator gearing used on Utility Helicopter math model	39
12	Effect of lateral center of gravity position on main rotor flapping in trimmed level flight	40
13	Effect of sideslip on main rotor flapping in trimmed level flight	41
14	Effect of dihedral on main rotor flapping in trimmed level flight	42
15	Effect of gross weight on main rotor flapping in trimmed level flight	45
16	Effect of rotor RPM on main rotor flapping in trimmed level flight	46
17	Effect of climbs and descents on main rotor flapping in trimmed flight	47

LIST OF ILLUSTRATIONS (Continued)

Figure		Page
18	Effect of hub restraint on main rotor flapping in trimmed level flight	49
19	Typical roller-coaster maneuver	60
20	Effect of hub restraint on low-g flapping in roller-coaster maneuver	66
21	Effect of minimum-g level in roller-coaster maneuver	67
22	Typical roll reversal maneuver	70
23	Typical autorotation entry maneuver	74
24	Typical tail rotor loss maneuver	78
25	Effect of control input magnitude and rate on main rotor flapping	81
26	Typical pop-up from hover	82
27	Typical hard landing and jump takeoff - SCAS on	84
28	Typical hard landing and jump takeoff - SCAS off	85
29	Sample mast shear and moment loads during flapping stop contact	92

LIST OF TABLES

Table		Page
1	TEETERING ROTOR FLAPPING RESPONSE DUE TO CONTROL RATES	28
2	ARTICULATED ROTOR FLAPPING RESPONSE DUE TO CONTROL RATES	29
3	EFFECT OF BLADE FLEXIBILITY ON AMPLITUDE OF TIP FLAPPING ANGLE FOR TEETERING ROTOR	51
4	EFFECT OF BLADE FLEXIBILITY ON AMPLITUDE OF HUB AND TIP FLAPPING ANGLES FOR ARTICULATED ROTOR	53
5	EFFECT OF BLADE FLEXIBILITY ON AMPLITUDE OF ROOT AND TIP FLAPPING ANGLES FOR HINGELESS ROTOR	53
6	GUST CHARACTERISTICS FOR SIMULATIONS	55
7	FLAPPING EXCURSIONS DUE TO GUSTS	56
8	FUSELAGE RATE AND ATTITUDE LIMITS	58
9	GROSS WEIGHT AND CG EFFECTS ON FLAPPING IN ROLLER-COASTER MANEUVER	63
10	EFFECT OF HUB RESTRAINT ON FLAPPING IN ROLLER-COASTER MANEUVER AT 140 KNOTS	65
11	FLAPPING IN ROLLER-COASTER MANEUVER FOR DIFFERENT HELICOPTER AND ROTOR TYPES	69
12	EFFECT OF HELICOPTER TYPE ON ROLL REVERSAL MANEUVER	71
13	EFFECT OF CENTER OF GRAVITY LOCATION ON RESPONSE TO LATERAL CONTROL INPUTS	73
14	FLAPPING IN AUTOROTATIONAL ENTRIES	76
15	FLAPPING IN TAIL ROTOR LOSS	79
16	FLAPPING IN HARD LANDINGS FROM HOVER	86

1. INTRODUCTION

A fundamental helicopter design consideration is rotor blade flapping. Flapping clearance with the fuselage and tail rotor are dictated by design parameters, such as mast length, fuselage layout, and rotor blade flapping stops. The many possible in-flight and ground operations require consideration of blade coning and flapping motions under a wide variety of operating conditions.

Current design criteria state that a minimum rotor blade to airframe clearance of 9 inches must be present to allow safe operations. However, with these criteria apparently satisfied, incidents caused by excessive flapping in all rotor types still occur in service.

The objectives of this study were to generate a general picture of flapping problems by defining the primary causes of high flapping and to formulate design criteria. The scope of the study included examining the effect of both physical and operational characteristics of three mission types of helicopters with four rotor systems and identifying differences in flapping characteristics.

1.1 CURRENT DESIGN CRITERIA

Current general helicopter design specifications, References 1 through 6, were examined for rotor blade flapping design criteria. These specifications addressed rotor blade clearances

---

[1]Anon., MILITARY SPECIFICATION - STRUCTURAL DESIGN REQUIREMENTS - HELICOPTERS, MIL-S-8698 (ASG), Naval Publications and Forms Center, Washington, D.C., Feb. 1958.

[2]Anon., STRUCTURAL DESIGN REQUIREMENTS (HELICOPTERS), AR-56, Naval Air Systems Command, Department of the Navy, Washington, D.C., Feb. 1970.

[3]Anon., ENGINEERING DESIGN HANDBOOK, HELICOPTER ENGINEERING, PART ONE: PRELIMINARY DESIGN AMCP 706-201, U.S. Army Materiel Command, Alexandria, Virginia, August 1974.

[4]Anon., GENERAL SPECIFICATION FOR DESIGN AND CONSTRUCTION OF AIRCRAFT WEAPON SYSTEMS, VOLUME II - ROTARY WING AIRCRAFT, SD-24K, Naval Air Systems Command, Department of the Navy, Washington, D.C., December 1971.

[5]Anon., CIVIL AIR REGULATIONS - PART 6 - ROTORCRAFT AIRWORTHINESS: NORMAL CATEGORY, Federal Aviation Administration, Department of Transportation, Washington, D.C., December 1966.

[6]Anon., FEDERAL AVIATION REGULATIONS, PART 27: AIRWORTHINESS STANDARDS: NORMAL CATEGORY ROTORCRAFT, Federal Aviation Administration, Department of Transportation, Washington, D.C., August 1974.

for both in-flight and ground operations, wind loads in starting or stopping the rotor, and rotor torque loads. Only Reference 3 addresses the problem of in-flight flapping stop contact and states that this condition must be avoided or, if it happens inadvertently, no components of primary importance to flight safety are to be damaged.

These specifications allow the rotor designer the latitude required for innovative design but do not provide guidance or a method of proof that flapping will cause no problems in any realm of flight. At present, lack of extreme flapping during the flight test and the structural demonstration qualification tests is considered to be sufficient proof that no flapping problems exist.

However, once the helicopter is in service, the variety of missions and operational maneuvers may uncover areas in which, despite the extensive tests by the manufacturer, the licensing agency, or the customer, flapping becomes a problem. Fuselage strikes, mast bumping, droop stop pounding, and high fatigue loads are all symptoms of excessive flapping that may not appear in qualification tests. Generally, these flapping problems arise when a helicopter is operated outside the recommended flight envelope or when components have failed. It is in these areas that adequate design criteria do not exist.

1.2 TECHNICAL APPROACH

The approach used in this study began with the development of simulation models of three helicopters and three rotor types. Then a parametric study was made using one of these helicopters to gain insight into the basic causes of excessive flapping. Pilot tolerances and physical capabilities were assessed to provide realistic maneuvering limits that were used in a simulation program of suspected critical flight conditions. From this simulation, a number of basic causes of high flapping were found. Using the results of this study and the current design specifications, a proposed new design criterion was formulated.

2. SIMULATION MODEL DEVELOPMENT

The basic functions of the main rotor are to provide lift, propulsion, and forces and moments to maintain trim or to change the equilibrium of the helicopter. The pilot controls the magnitude and orientation of the rotor forces and moments with the cyclic and collective controls.

The individual rotor blades generate forces and moments as they rotate about the rotor shaft. To maintain equilibrium the blades must create approximately the same thrust at all times in their sweep around the shaft; thus, in all but hovering flight, the unequal velocities of the advancing and retreating blades require flapping to adjust the blade angle of attack to maintain this constant thrust. Since the thrust produced by each blade is approximately equal around the disk, the thrust vector will be approximately perpendicular to the disk. Therefore, changes in flapping relate to changes in the orientation of rotor thrust and hub moments required to balance the helicopter.

2.1 GENERAL FLAPPING DESCRIPTION

A rotor blade mounted on a mast may be represented as an elastic beam hinged near or on the mast centerline. The hinge may be in the form of a teetering pin, a flapping hinge, or an apparent hinge for hingeless rotors. The rotor system may have a set precone angle with respect to the mast. In addition, the mast will be mounted through a pylon system which may tilt with respect to the fuselage waterline (horizontal plane in the body axis). These relations are illustrated in Figure 1.

Two ways of looking at flapping are apparent from this figure. If the clearance between the rotor blade and the airframe is of interest, knowledge of the deflection of the blade relative to the fuselage is needed. If clearance at the flapping stop or the hub bending moments are of interest, the hub flapping angle with respect to the shaft axis is important. Both these aspects of flapping are also functions of the shaft tilt from its nominal setting.

In steady flight, the shaft will generally tilt in the direction tending to relieve flapping; i.e., forward tilt with down forward flapping. However, in maneuvers involving rapid multiple cyclic control inputs, it may be possible to get the pylon to tilt in a direction tending to increase shaft angle flapping.

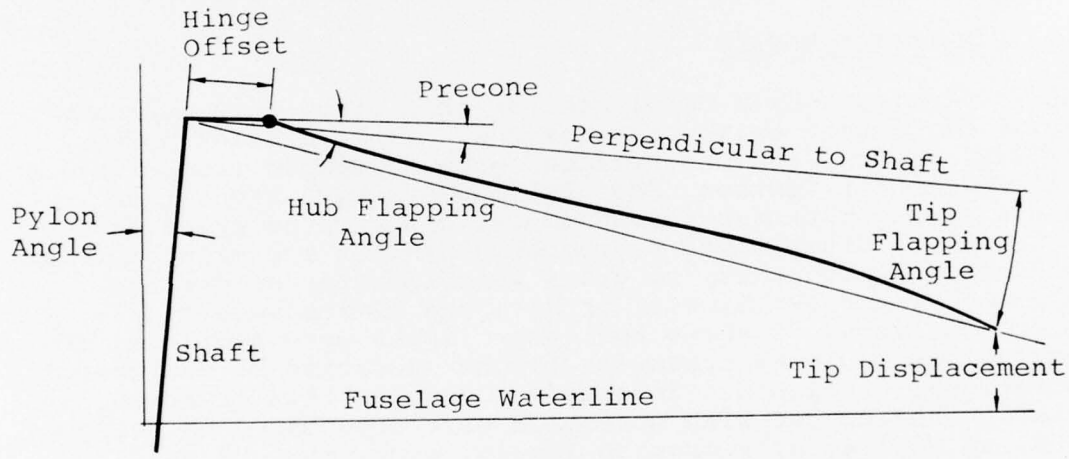

Figure 1. Spanwise view of elastic rotor blade.

Since this study uses fictitious helicopters and the pylon support system dynamics are unique for each helicopter, the rigid pylon was considered to be rigidly attached to the fuselage at all times. This simplification provided flapping values unaffected by uncertain pylon dynamics. However, when applied to actual helicopters, full pylon representation should be used.

When considering rotor out-of-plane displacements, the pitch of the blade at a particular azimuth becomes important. From Figure 2, the trailing edge of the blade is seen to be the lowest point on the blade. With blade twist generally lower at the tip, the pitch near the hub (and consequently nearest the fuselage pylon area) is more positive, and the minimum out-of-plane deflections are the lowest. The calculation of flapping to determine adequate fuselage clearance must therefore include collective pitch.

2.2 SIMULATION MODELS

The simulation models developed for this study were representative of current helicopter designs. Three mission types, utility, attack, and observation, were developed from existing Bell Helicopter Textron (BHT) helicopters with simplified fuselage and empennage aerodynamics, and with no pylon degrees of freedom. Since these helicopters did not represent actual production helicopters, no gross weight/center of gravity envelope, rotor RPM limits, or airspeed limits were available. Estimates of these and other limits were made, but no conclusions could be drawn for flight operation beyond normal operational envelopes. In order to examine this question, an existing helicopter with operation envelopes based on fatigue, handling qualities, vibration levels, etc., must be used.

Four types of rotor systems were used on the utility type helicopter. These were two-bladed teetering rotors with and without hub restraint and four-bladed rotors with articulated and hingeless hub types. In order to compare these rotor types, the blade radius and operating rotor rpm were unchanged and the Lock numbers of the blades were held constant.

The simulation of the critical flight condition used the C81 Rotorcraft Simulation Program (Reference 7). The BHT hybrid computer version of this program was used, which placed some limitations on the rotor representation. Hybrid C81 is restricted to rigid, centrally hinged blades with equations used

---

[8] J. M. Davis, et al, ROTORCRAFT FLIGHT SIMULATION WITH AEROELASTIC ROTOR AND IMPROVED AERODYNAMIC REPRESENTATION, USAAMRDL Technical Report 74-10A, B, C, Eustis Directorate, U.S. Army Air Mobility Research and Development Laboratory, Fort Eustis, Virginia, June 1974, AD 782854, 782756, and 782841.

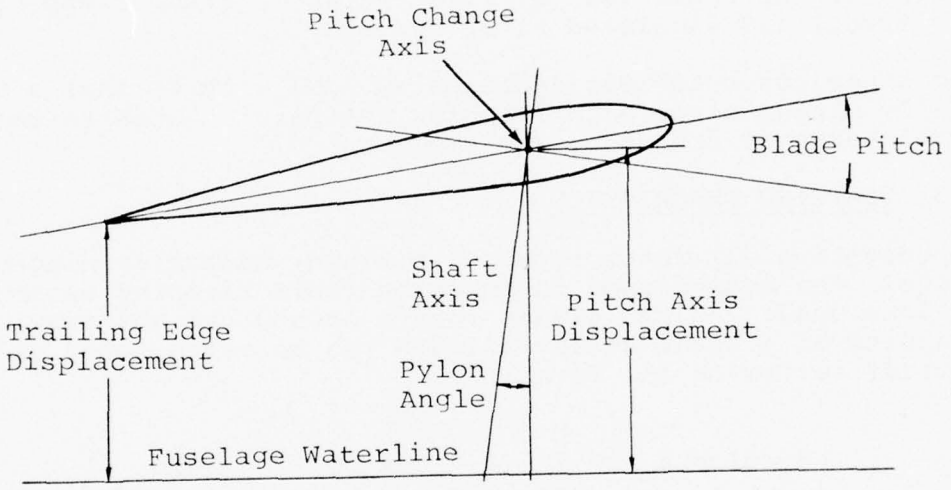

Figure 2. Rotor blade displacement.

for rotor aerodynamics. The rotor systems were modeled as illustrated in Figure 3. The two-bladed teetering rotor is represented with a centrally located teetering pin and a rigid hub with underslinging and precone. This allows moment carry-over from one blade to the other, similar to what exists in the actual rotor system.

The articulated rotor with offset flapping hinges could not be represented as exactly on the hybrid version of C81. This rotor was modeled as four independent blades that are centrally hinged with flapping restraint springs chosen to match the flap-wise natural frequency of the articulated rotor. When the flap-wise natural frequencies are matched, the modeled blades will respond to first harmonic excitation the same as the actual articulated blades. The simulation is considered to be ade-quate for the comparison of first harmonic blade flapping of the actual and simulated rotor systems.

The hingeless rotor was represented similarly in that a cen-trally hinged blade with flapping restraint chosen to match the first harmonic frequency was used.

2.3 FLAPPING DESCRIPTION

Representing all rotor types with rigid, centrally hinged rotor blades, the method used to describe their flapping motion will be developed. As the blades rotate around the shaft axis, the flapping of a blade at any azimuth can be represented using a Fourier series of the form

$$\beta_s(\psi) = a_{o_s} - \sum_{n=1}^{N} (a_{n_s} \cos n\psi + b_{n_s} \sin \psi)$$

where N is the number of harmonics to be used.

If only the first harmonic (one-per-rev) is used, N=1 and the equation can be written as

$$\beta_s(\psi) = a_{o_s} - a_{1_s} \cos \psi = b_{1_s} \sin \psi$$

or

$$\beta_x(\psi) = a_{o_s} - c_{1_s} \cos(\psi - \phi)$$

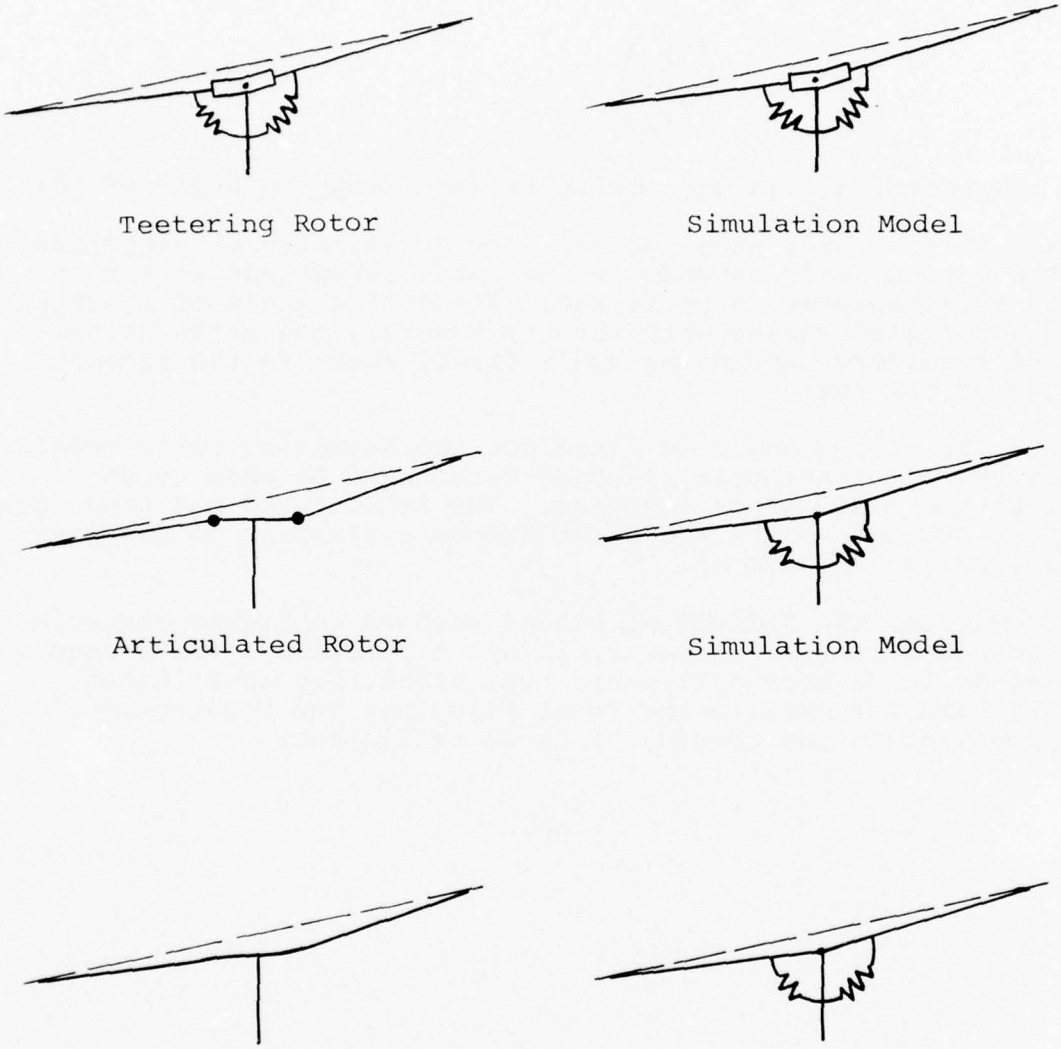

Figure 3. Mathematical models of blade quarter chord lines used in hybrid C81.

where

$$c_{1_s} = \sqrt{a_{1_s}^2 + b_{1_s}^2}$$

$$\phi = \tan^{-1}\left(\frac{b_{1_s}}{a_{1_s}}\right)$$

In this form, a_{o_s} is the coning or mean flapping angle of the blade in the shaft axis system. The articulated or hingeless rotor coning angle depends on the rotor thrust and will thus vary as a maneuver is performed. The coning angle of a teetering rotor also varies with thrust; however, the mathematical model considers the coning angle fixed, equal to the precone angle of the hub.

Since the coning angle is fixed for the teetering rotor models, only the first-harmonic flapping terms need be used to describe the rigid blade flapping. The articulated and hingeless rotors require coning and first harmonic flapping to describe blade motion (Figure 4).

In addition, the individual blades respond to higher harmonic aerodynamic inputs. However, in all simulations, the second-harmonic terms were noticeable but, since they contributed only a small amount to the total flapping, the first-harmonic representation was considered to be sufficient.

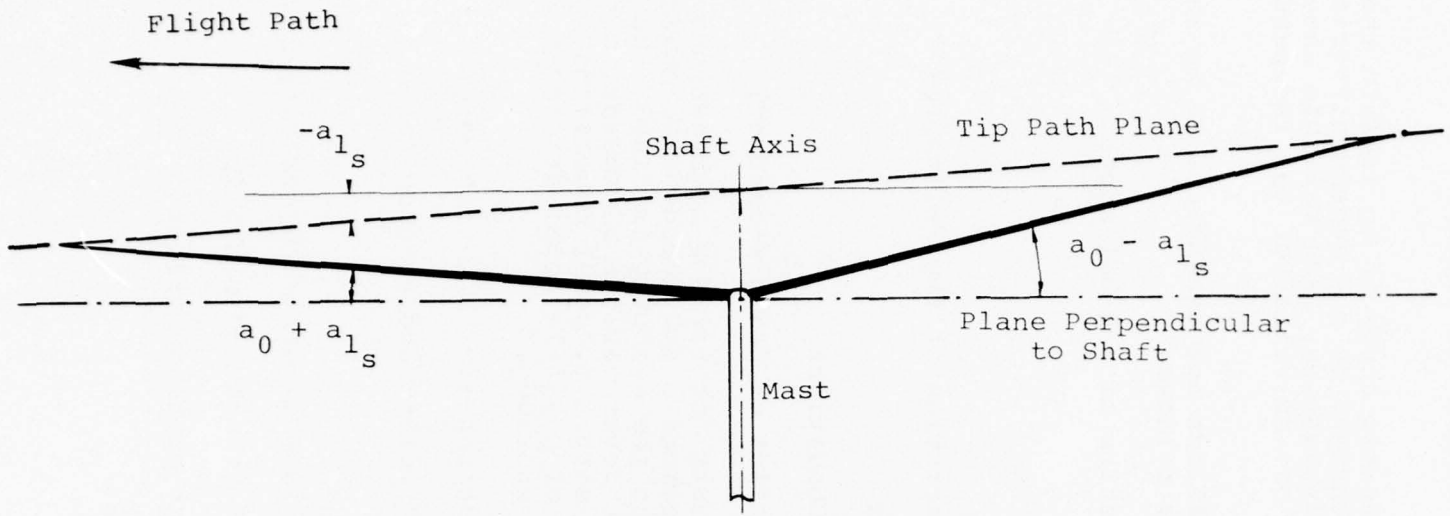

Figure 4. Shaft Axis flapping for longitudinal flapping and coning only.

3. PARAMETRIC STUDY

The basic idea of a parametric study is to isolate the effects of independent variable changes on the dependent variable to be investigated. To be exhaustive, each variable should be checked for all combinations of values of the independent variables.

For this study, the conditions and parameters to be investigated are classified as follows:

Physical Characteristics of the Helicopter

- Rotor
- Airframe

Operational Characteristics of the Helicopter

- Flight Conditions
- Rotor Operating Conditions
- Control Inputs (pilot or failure-induced)

This classification accounts for various combinations of airframe and rotor system geometric and aerodynamic characteristics that are compatible. Once the geometry is fixed, the variety of flight conditions must cover various airspeeds, altitudes, angular rates, rotor RPM settings, power conditions, control inputs, etc. The matrix of possible combinations of these independent variables is enormous.

The specific parameters chosen for this work were:

- Rotor thrust coefficient and advance ratio
- Control inputs
- Longitudinal and lateral center of gravity location
- Fuselage angle of attack and sideslip
- Flapping restraint or hinge offset
- Blade flexibility
- Gusts

These factors were picked based on flight experience, test results, and analytical studies as being significant contributors to high flapping magnitudes.

3.1 ISOLATED ROTOR ANALYSIS

The first portion of the parametric study was for the rotor isolated from the helicopter, as in a wind tunnel. The forces and moments generated by the rotor are simply reacted to by the mast with no mast displacement allowed.

Initially, a simplified analysis was developed to provide a means of predicting flapping trends with equations whose individual terms could be examined to show the effects of various parameters on flapping. Various types of two-bladed and four-bladed rotor systems were simulated; however, even with a set of simplifying assumptions, the derivation produced a set of five simultaneous equations for a hingeless or articulated rotor system and two simultaneous equations for a two-bladed teetering rotor system. This makes it very difficult to make a judgement by observation on what effect a single parameter might have on flapping.

These simplified equations were solved with a digital computer program, and sweeps of flapping springs, flapping hinge offset, shaft angle, velocity and thrust coefficient to solidity ratio (C_T/σ) were made. The flapping trends for these parameters looked reasonable, but when similar configurations were run in C81, the magnitudes of the total flapping angle were much higher than the simplified analysis showed. This was partly due to the lower collective pitch angles that the simplified analysis calculated to obtain the same C_T/σ. Also, the analysis assumed no stall, uniform inflow, a negligible radial component of the resultant air velocity, a simplified expression for the induced velocity that is independent of flapping, and a collective pitch angle necessary to provide a specified C_T/σ that is independent of flapping. These assumptions are not in C81, and it is believed that this is the cause of the low flapping angles calculated by the analysis, especially at high values of C_T/σ and advance ratio.

The discrepancies between C81 and this simplified analysis were too large to allow confidence in the analysis for the parametric investigations. To improve the analysis would require the elimination of the stated assumptions, but this would complicate the method to a degree near that of C81. Therefore, the effort for a simplified analysis was dropped in favor of the digital C81 computer program.

3.1.1 Rotor Simulation Results

The six rotor configurations described earlier were used in the wind tunnel mode of digital C81. Computer runs were made varying the advance ratio, C_T/σ, the shaft angle, and the flapping hinge offset or the flapping restraint when applicable. The cyclic controls were set to zero, and the collective pitch was swept to cover a range of C_T/σ for a given shaft angle and velocity. All of the rotor configurations showed a linear increase in down aft flapping with an increasing advance ratio for unstalled rotor conditions. The lateral flapping started down right at low advance ratios and shifted slightly upward as the advance ratio increased. As the collective pitch was increased, which increased C_T/σ, the down aft flapping grew larger and the down right lateral flapping showed a slight increase. When the combination of advance ratio and C_T/σ became large enough to introduce a stalled condition, the down aft flapping grew sharply and the lateral flapping began to shift toward down left. These trends continued as the rotor went deeper into stall. Changes in the shaft angle only altered the magnitude of C_T/σ for a given collective pitch, but there was no change in the flapping trends.

Figure 5 illustrates the effect of the rotor thrust coefficient on the total flapping angle in this wind tunnel mode. When retreating blade stall is reached, the increase in blade flapping is quite apparent. These results are for a rotor operating in steady conditions. In maneuvers, the angular rates developed on the helicopter will change the thrust coefficient for this blade stall effect. In particular, the positive pitch rates seen while maneuvering at high load factors can increase the thrust coefficient at stall significantly, as reported in Reference 8.

Flapping hinge offset and restraint were varied for the hingeless and articulated rotors, and changes in flapping restraint were also introduced to the utility two-bladed rotor configuration. However, since these rotors were in the wind tunnel mode, which fixes the shaft angle regardless of the loads transmitted to it, there was very little change in flapping. This is because realistic values of hinge offset and restraint only change the first out-of-plane natural frequency from 1 per rev to values less than 1.1 per rev. Since the flapping determined in the

---

[8] E. L. Brown and P. S. Schmidt, THE EFFECT OF HELICOPTER PITCHING VELOCITY ON ROTOR LIFT CAPABILITY, Journal of the American Helicopter Society, Vol. 8, No. 4, October 1963.

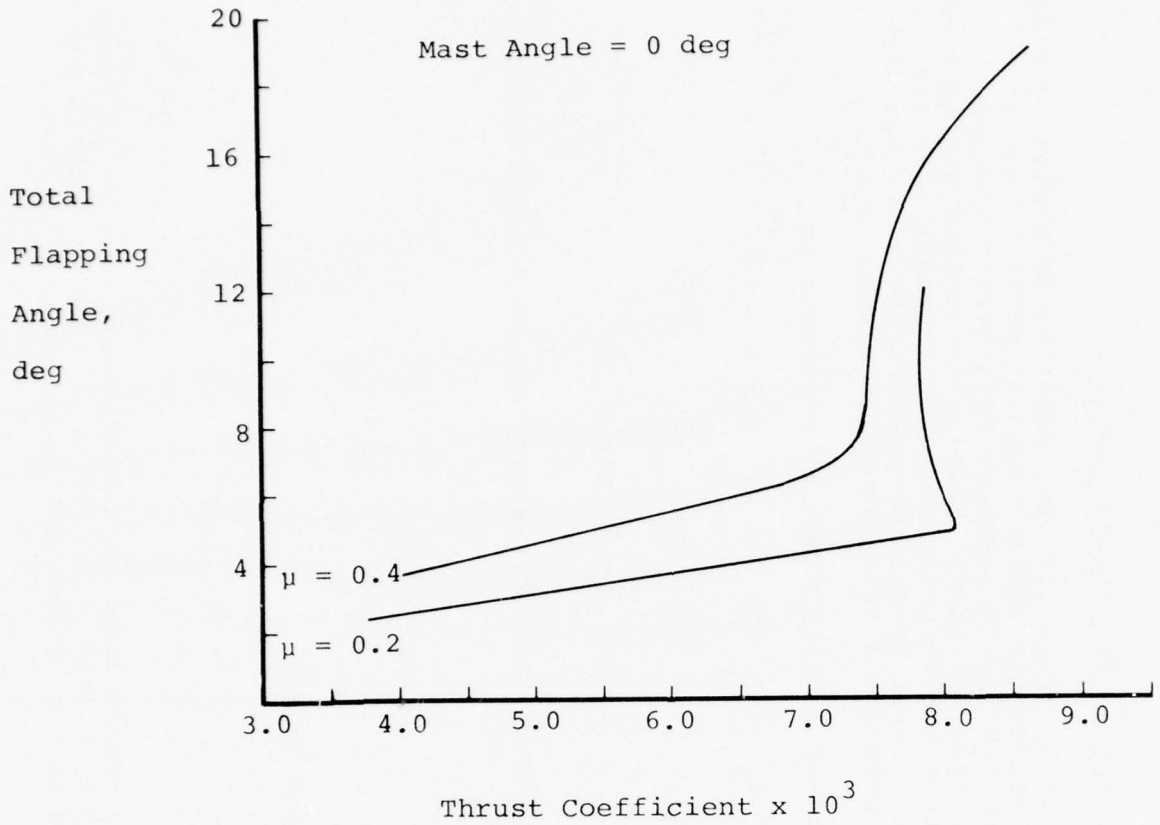

Figure 5. Effect of thrust coefficient on rotor flapping.

wind tunnel mode is simply the forced dynamic response, these small changes in the flapping frequency produce small changes in flapping response even though the loads transmitted to the shaft may vary by a large amount. All six rotor configurations showed basically the same flapping trends in the wind tunnel mode with the cyclic pitch controls set to zero. The main observation is that the down aft flapping grows at a rapid rate, and the lateral flapping shifts toward down left when the rotor is driven into stall.

3.1.2 Control Inputs and Angular Rates

Swashplate control inputs are very powerful in producing flapping with respect to the shaft. Angular rates of rotation about the rotor hub in the pitch or roll directions also generate shaft axis flapping. Simple expressions are available in the literature for flapping caused by changes in these parameters for a rotor mounted on a shaft that does not displace due to rotor loads as it would in a wind tunnel.

If the flapping of a rotor blade is expressed as

$$\beta_s = a_o - a_{1_s} \cos \psi - b_{1_s} \sin \psi$$

and the pitch as

$$\theta = A_o - A_1 \cos \psi - B_1 \sin \psi$$

then an approximation of the flapping due to a longitudinal swashplate input is

$$\frac{\partial a_{1_s}}{\partial B_1} = - (1 + 2.2\mu^2)$$

and for a lateral input,

$$\frac{\partial b_{1_s}}{\partial A_1} = 1$$

These equations approximate the steady-state changes in rotor flapping due to a control input for a helicopter that is not free to respond to the forces and moments resulting from these inputs.

The transient response to a step control input can be approximated using the rotor lag equations (Reference 9):

$$\frac{\partial a_{1_s}}{\partial q} = \frac{16}{\gamma\Omega}\left(\frac{1}{1 - \frac{1}{2}\mu^2}\right)$$

and

$$\frac{\partial b_{1_s}}{\partial q} = \frac{16}{\gamma\Omega}\left(\frac{1}{1 + \frac{1}{2}\mu^2}\right)$$

The approximate change in longitudinal rotor flapping due to a longitudinal step input in cyclic pitch is

$$\Delta a_{1_s} = -\frac{\partial a_{1_s}}{\partial B_1}\,\Delta B_1\left[1 - e^{-\frac{t}{\tau}}\right] \text{ where } \tau = \frac{\partial a_{1_s}}{\partial q}$$

This assumes that the aerodynamic forces are much greater than the blade inertial forces, which allows us to assume that the rotor can be represented as a first order rather than a second order system. This is a reasonable approximation only as long as the damping is large, as it is in most rotor systems.

An example of this first order response is shown in Figure 6 for a rotor in flat pitch.

It is noticed that, with this assumption, no overshoot is seen even with the instantaneous control input. This phenomenon was verified on the hybrid simulation and, for example, in test measurements on an actual helicopter, as reported in Reference 10.

Two methods were used to assess the effects of control input rates on flapping. In the first, a teetering and articulated rotor were each simulated in the wind-tunnel mode of digital C81 at 140 knots, sea level standard day conditions. The teetering rotor was modeled with a rigid hub attached to flapwise

---

[9]K. B. Amer, THEORY OF HELICOPTER DAMPING IN PITCH OR ROLL AND A COMPARISON WITH FLIGHT MEASUREMENTS, Technical Note 2136, NACA, October 1950.

[10]R. H. Springer and D. Berger, CATEGORY II PERFORMANCE TEST OF THE UH-1J HELICOPTER, VOLUME II, Technical Report No. 72-17, U.S. Air Force Flight Test Center, Edwards AFB, Calif., May 1972.

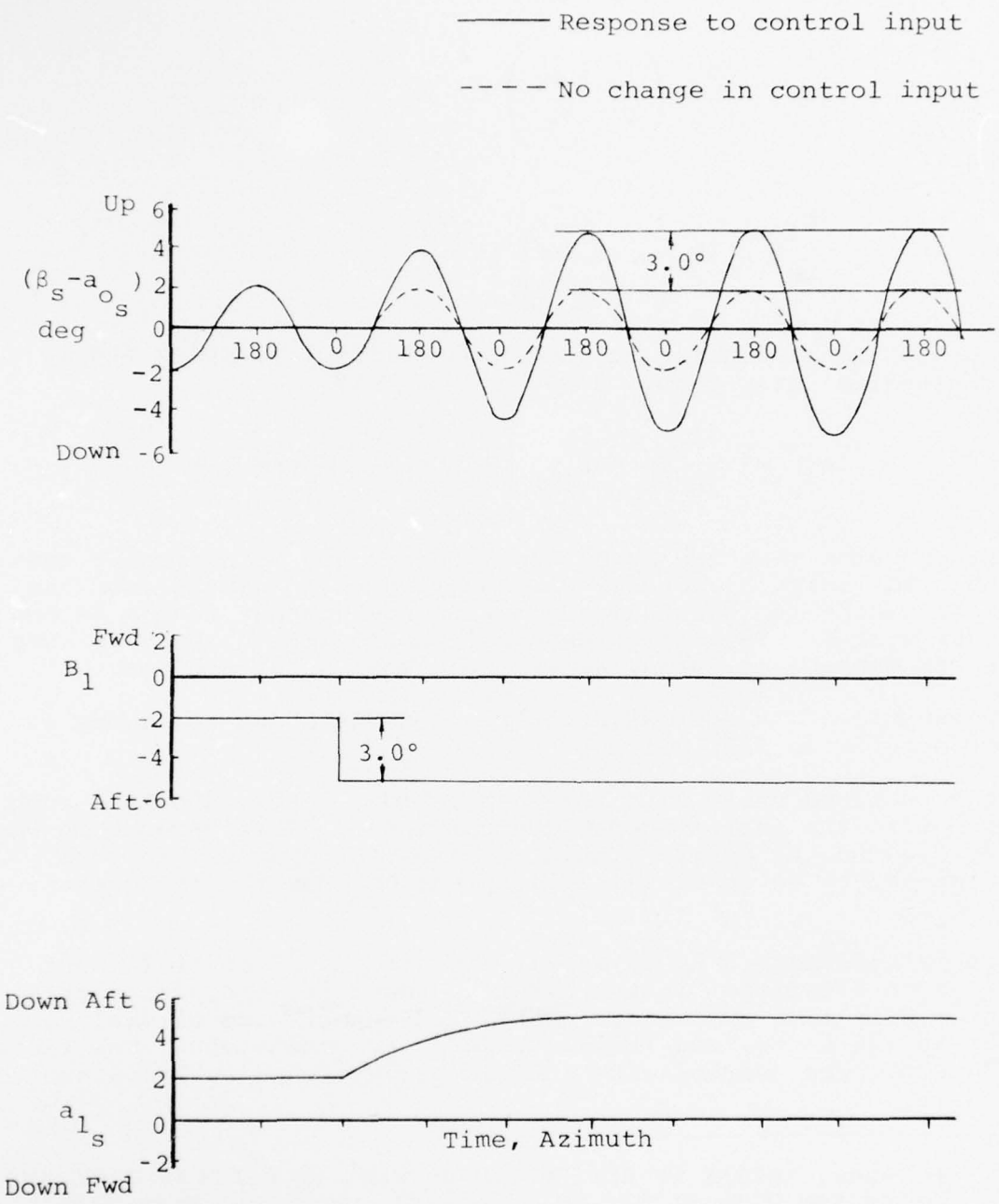

Figure 6. Flapping response to aft cyclic pitch step input.

flexible blades. The articulated rotor used rigid blades with both flapping and lead-lag hinges. The mast angle was chosen to correspond to the trimmed mast angle for the aircraft at 140 knots. Each of the three rotor controls (collective, longitudinal cyclic and lateral cyclic) were moved independently to determine the flapping due to varying control rates. The prescribed control motion was:

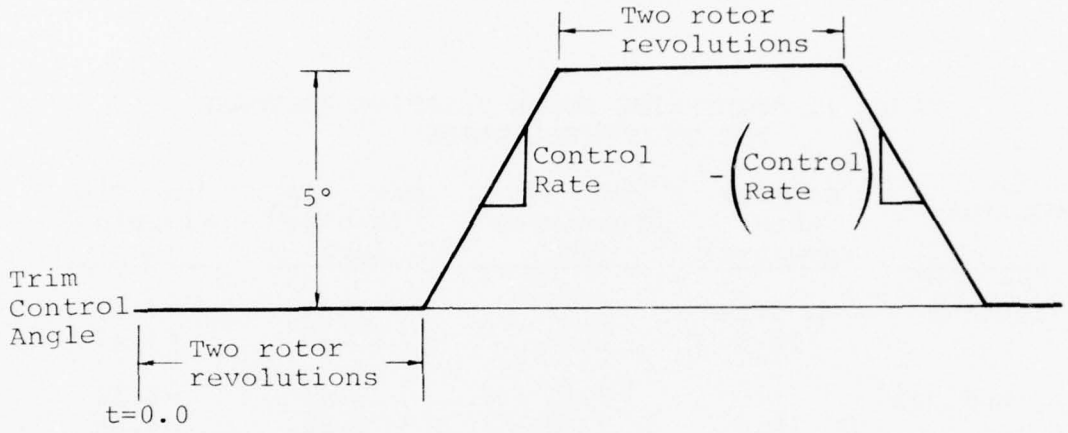

The control rates were 5.0 deg/sec and 10.0 deg/sec, with the results given in Tables 1 and 2. As can be seen, doubling the control rates caused no appreciable change in the flapping for cyclic or collective inputs.

The second method involved a series of control inputs in the wind tunnel mode of hybrid C81, using the teetering-rotor utility helicopter model. Control input times, t_o, from 0.01 to 1.0 sec were used to apply inputs of the form:

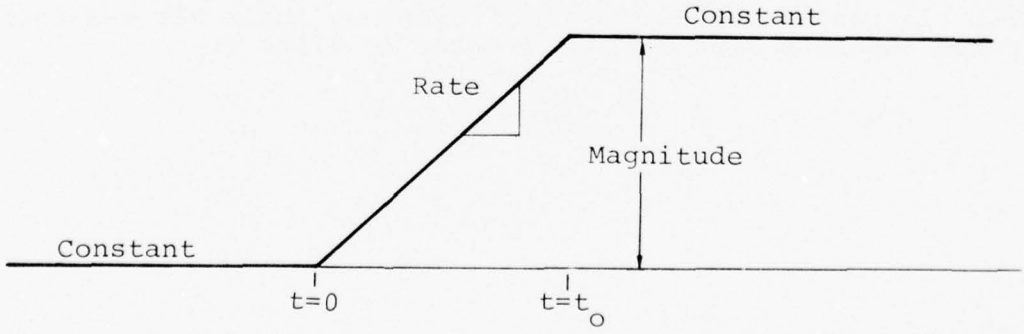

In all cases, the flapping increased to its steady-state value after the control input with no overshoot. At the higher control rates where the time required to apply the input was on the order of the time of a rotor revolution, the azimuth

TABLE 1. TEETERING ROTOR FLAPPING RESPONSE DUE TO CONTROL RATES

Control	Control Rate[1] (deg/sec)	Max. Hub Teetering[2] (deg)	Max. Tip Flapping[3] (deg)	Min. Tip Flapping[3] (deg)
Collective	5.0	7.36	11.34	-4.39
	10.0	7.48	11.49	-4.62
Longitudinal Cyclic	5.0	7.15	8.41	-6.12
	10.0	7.62	8.90	-6.59
Lateral Cyclic	5.0	4.49	6.79	-2.54
	10.0	4.56	6.90	-2.56
Steady flight value		1.33	3.64	0.65

[1]Positive Control Rates: Collective-Up, Longitudinal-Forward, Lateral-Right.

[2]Teetering = Motion of Rigid Body Hub About Teetering Pin

[3]Tip Flapping Includes Precone; Formed by Angle Between Shaft Plane and Line From Center of Rotor to Blade Tip

TABLE 2. ARTICULATED ROTOR FLAPPING RESPONSE DUE TO CONTROL RATES

Control	Control Rate[1] (deg/sec)	Max. Root Flapping[2] (deg)	Min. Root Flapping[2] (deg)	Max. Tip Flapping[3] (deg)	Min. Tip Flapping[3] (deg)
Collective	5.0	9.98	-4.18	9.55	-4.28
	10.0	10.38	-4.52	9.94	-4.62
Longitudinal Cyclic	5.0	7.32	-5.35	6.94	-5.42
	10.0	7.37	-5.64	6.99	-5.72
Lateral Cyclic	5.0	6.92	-1.67	6.55	-1.83
	10.0	7.13	-1.83	6.76	-1.99
Steady Flight Values		3.06	1.58	2.79	1.39

[1]Positive Control Rates: Collective-Up, Longitudinal-Forward, Lateral-Right.

[2]Root Flapping = Angle Between Shaft Plane and Straight Line From Flapping Hinge Pin (5% Radius) and Blade at 10% Radius

[3]Tip Flapping = Angle Between Shaft Plane and Line from Center of Rotor to Blade Tip.

position of the rotor where the step was applied became important. If input was made with the blade in a favorable position, the steady-state flapping would be reached faster than at other azimuths.

3.1.3 Effect of Operating Conditions

Under normal operating conditions, the rotor possesses sufficient damping not to overshoot the amount of flapping commanded by swashplate inputs. However, the flapping response equations will allow evaluation of some of the effects of other parameters on flapping due to control inputs.

Consider first the effect of reduced rotor rpm at constant airspeed. Since we are considering transient maneuvers, rpm values much lower than those which would sustain level flight may be seen.

Longitudinal flapping due to longitudinal swashplate inputs is a function of μ^2 and will cause an increase in flapping with reduced rotor rpm. This effect isn't significant except at very low rotor speeds, on the order of half the normal rpm, and in this condition, rotor stall effects may dominate. However, the effect of rotor rpm on rotor response is much more direct. An rpm decrease will decrease $\frac{\partial a_{1_s}}{\partial q}$ so that the rotor will reach its commanded position faster.

The rotor response term is also affected by parameters in the Lock number.

$$\gamma = \frac{\rho a c R^4}{I_b} = \rho a \left(\frac{c R^4}{I_b}\right)$$

High density altitudes will reduce the Lock number, which will in turn lengthen the response time of the rotor. In addition, changes in the blade lift curve slope due to blade stall or changes in operating Mach number will also affect the Lock number.

When the following parameters are varied independently for an unstalled rotor, rpm decrease leads to:

- An increase in longitudinal flapping caused by longitudinal control inputs
- No change in lateral flapping caused by lateral control inputs

- An increase in rotor damping caused by a longer response time

Density decrease leads to:

- No effect on flapping caused by control inputs
- An increase in rotor damping caused by a longer response time

Once blade stall becomes significant, no simple means exists to predict this effect. The blade average lift curve slope will decrease as the blade stalls, increasing the rotor following time. Retreating blade stall also contributes some down aft flapping caused by loss of lift on the blade at $\psi = 270°$.

Another effect that may be present is the reduction of pitch and roll damping in conditions of high thrust and high inflow velocities (Reference 9). This condition is typically found in a high-power climb at low airspeeds and will cause a loss of stability, requiring control inputs to maintain control.

In summary, the variations in flapping response due to control inputs are predicted well by classical theory except where blade stall is significant. The trends calculated using the hybrid and the digital versions of C81 agree well with simple theory.

3.2 ROTOR AND FUSELAGE COMBINED

The remaining parameters for investigation require the combination of the rotor and a fuselage to account for flapping in trimmed flight. In order to present the flapping information in an easily pictured form, a polar plot representation of flapping is used.

If the centrally hinged blades are described by the first harmonic flapping terms, the tip of the blades may be described as rotating in a plane that is tilted from a plane perpendicular to the shaft. Figure 7 illustrates a tip path plane tilted down aft by a_{1_s} degrees and down right by b_{1_s} degrees from the plane perpendicular to the shaft. Since the tip path plane is represented by only the first harmonic terms, this plane may be described as

$$\beta_s = - a_{1_s} \cos \psi - b_{1_s} \sin \psi$$

which will also describe a blade flapping angle with respect to the rotor shaft.

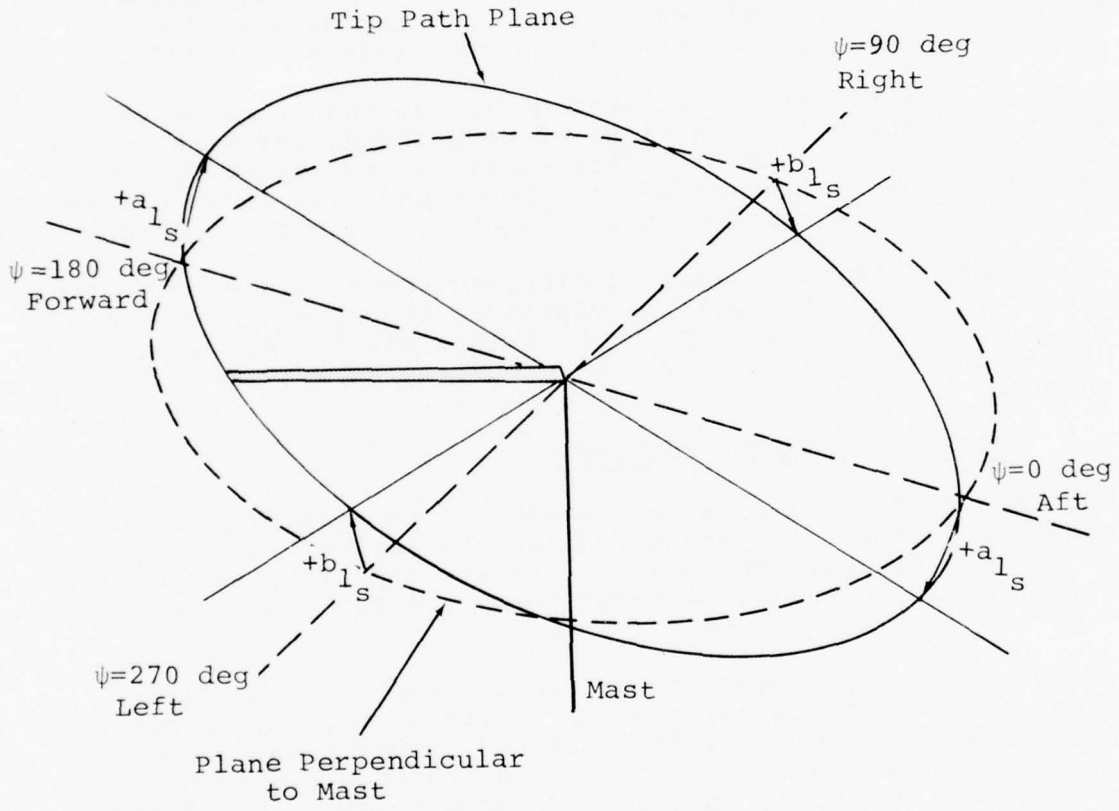

Figure 7. Tip path plane in shaft axis system.

It is difficult to picture the disk in this form when presenting flapping data, and a preferred representation is found if the above equation is converted to polar form:

$$\beta_s = - c_{l_s} \cos (\psi - \phi)$$

where

$$c_{l_s} = \sqrt{a_{l_s}^2 + b_{l_s}^2}$$

and

$$\phi = \arctan \left(\frac{b_{l_s}}{a_{l_s}} \right)$$

Thus, c_{l_s} is the maximum magnitude of shaft axis flapping, and ϕ is the azimuth position at which the maximum down flapping occurs. In this form, the flapping in a given condition may be plotted in polar form where the radial distance corresponds to the flapping magnitude and the angular coordinate corresponds to the azimuth.

Digital C81 was used to generate a series of trimmed-flight conditions for the entire helicopter (rotor and airframe) in which the shaft axis flapping coefficients were calculated.

3.2.1 Baseline Helicopter Flapping

Figure 8 shows the flapping trend for the baseline utility helicopter at a mid-gross weight and a neutral center of gravity location. Analysis of this plot will indicate some basic characteristics of the helicopter and will provide a base on which the parametric study will rest. Starting at hover, the flapping is about 2° down aft and left. The left flapping is expected because of the left tilt of the main rotor thrust vector that is required to balance the tail rotor thrust, which is to the right.

As rearward flight is entered, a large down aft flapping change of about 4° is seen, primarily because of the elevator configuration used for this helicopter. A tail-boom-mounted elevator at about 75% rotor radius will receive the full impact of main rotor downwash in hover, causing a significant download. As rearward flight is entered, the rotor wake will gradually sweep forward of the elevator, and when free of this wake, the elevator download will diminish significantly, providing a nose-down pitching moment that will cause the tail of the aircraft to rise. As no significant change in the rotor thrust vector tilt is required to account for this change, its orientation

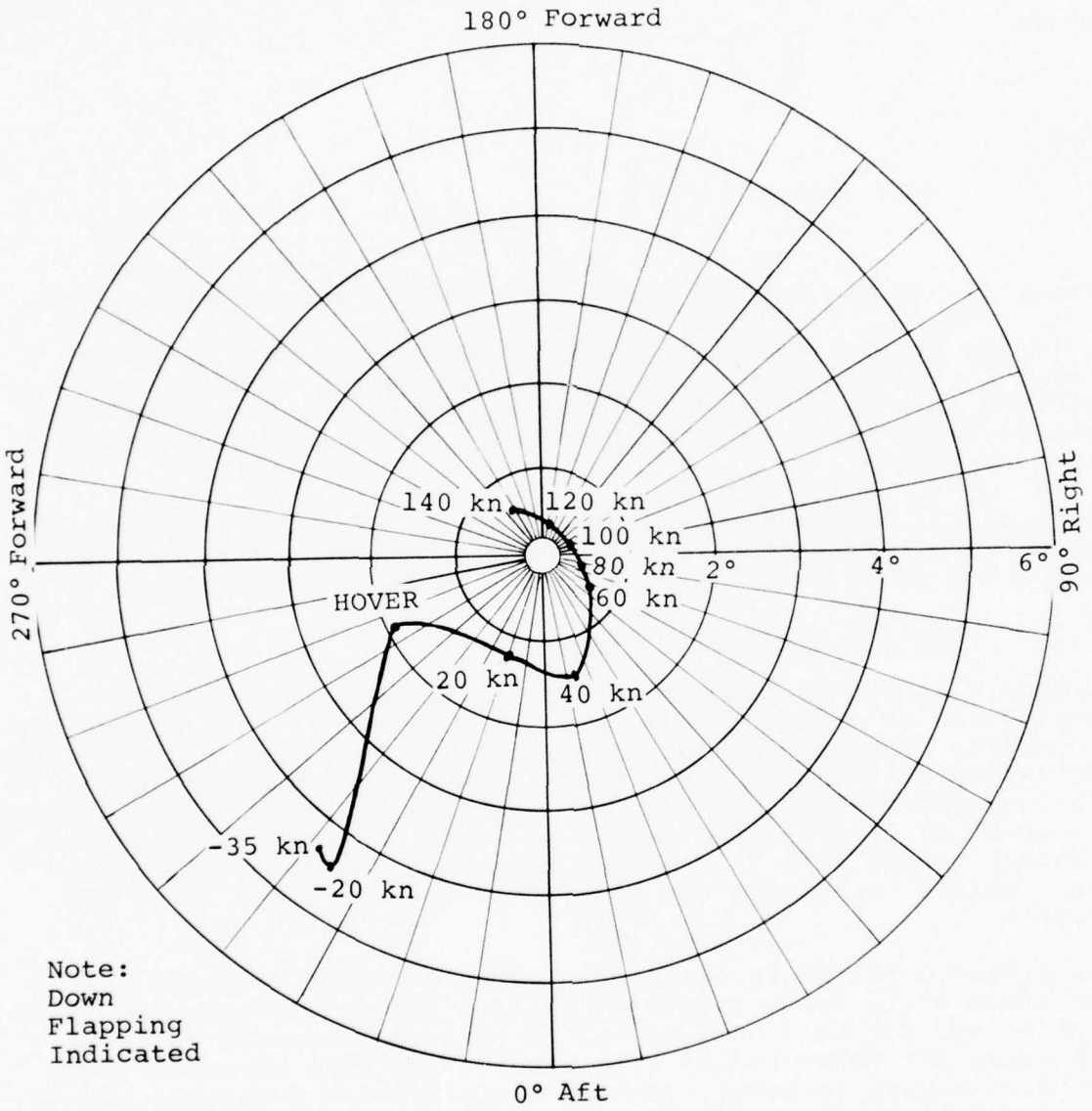

Figure 8. Polar plot of main rotor flapping in trimmed level flight.

in space will remain approximately the same, and the pilot will be required to provide aft cyclic swashplate tilt to maintain rearward flight. The rotor will thus flap aft with respect to the rotor shaft. It is apparent that, if the elevator were not mounted on the tailboom in this manner, this aft flapping in rearward flight would not be as pronounced.

From hover to forward flight, we see a change in flapping that is primarily down right. Part of this is due to a reduction in the tail rotor thrust required, and part is due to the curved inflow effect, which will cause down right flapping for slow forward flight. As speed is increased, the flapping trend is down forward and left, reflecting the increasing thrust vector forward tilt to counteract the drag at higher speeds and the increased side force from the fin and tail rotor that is required as main rotor torque is increased. As will be discussed, the flapping at high speed is a strong function of the pitch stability of the aircraft.

Figure 9 presents the flapping trends of the baseline helicopter for right and left sideward flight. In right sideward flight, almost pure down aft flapping occurs between hover and about 30 knots. This trend occurs because: (1) the distorted inflow at low advance ratio causes flapping about an axis at 90 degrees to the direction of flight (Reference 11), and (2) down aft flapping is caused by the reduced elevator download because of a lower induced velocity from the main rotor as airspeed is increased from hover. In addition, on some helicopters with conventional main rotor direction of rotation (counterclockwise as viewed from above), the tail rotor thrust provides a propulsive force to the right that keeps the fuselage roll attitude near level at speeds below about 30 knots. At higher speeds, a tendency for the rotor wake to sweep off of the elevator, giving an additional nose down pitching moment, will exist that may also give more down aft flapping. This effect has been verified experimentally on a BHT gunship.

For left sideward flight, the low advance ratio inflow effect tends to make the rotor flap down forward, and the reduced download on the elevator with increased speed gives down aft flapping, resulting in less total flapping change since these effects oppose each other.

3.2.2 Center of Gravity Location Effect

The fuselage longitudinal and lateral center of gravity (cg) location is a powerful factor affecting flapping. Cg location

---

[11] F. D. Harris, ARTICULATED ROTOR BLADE FLAPPING MOTION AT LOW ADVANCE RATIO, Journal of the American Helicopter Society, Vol. 17, No. 1, January 1972, pp. 41-48.

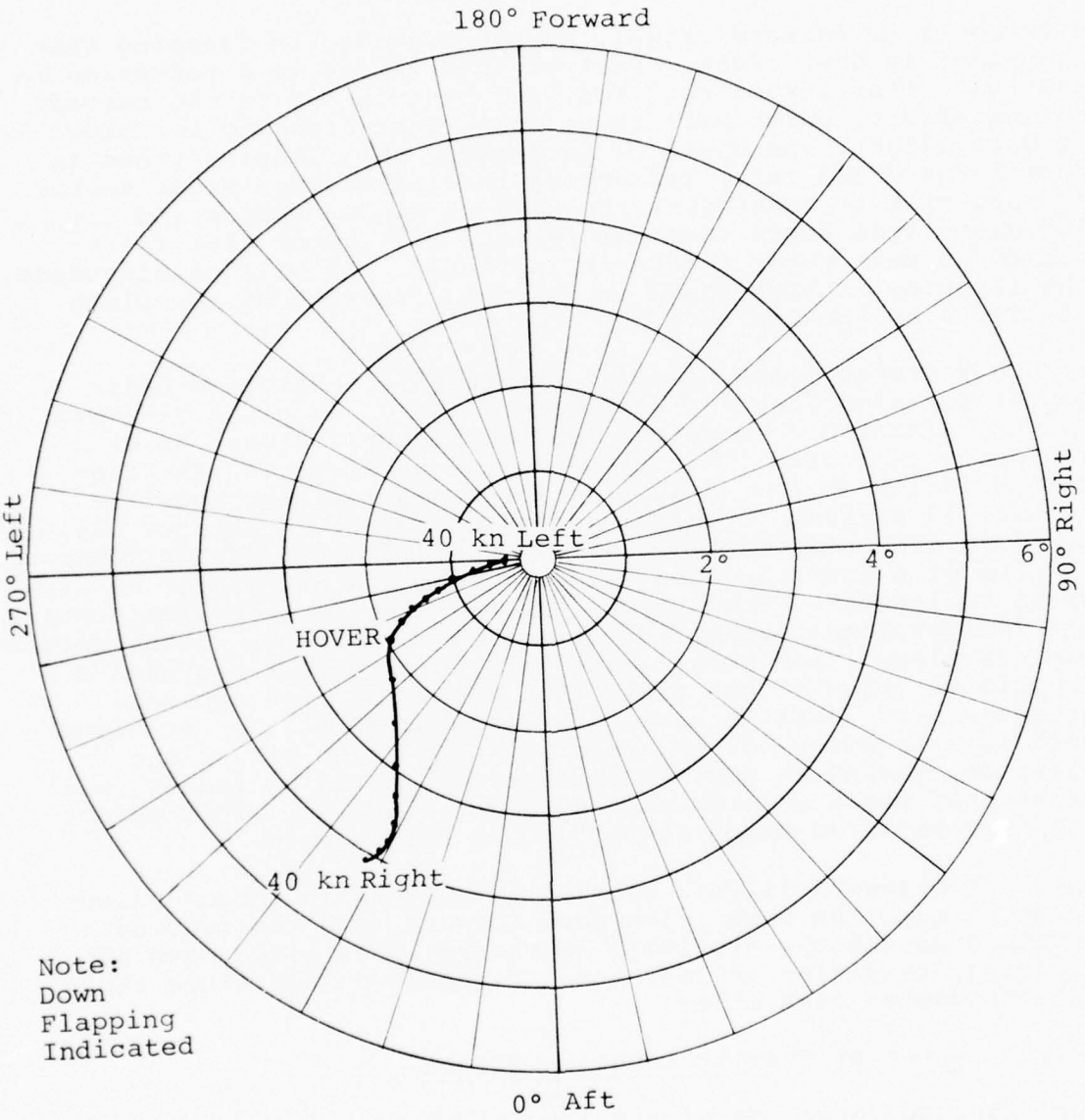

Figure 9. Effect of sideward flight velocity on main rotor flapping in trimmed level flight.

impacts on both the pitch or roll attitude of the ship in hover and on the pitch stability of the aircraft. Another factor is the effect on control margins in flight that may provide a limit to attainable airspeed in a given direction.

Figure 10 shows the effect of a longitudinal cg shift in forward and rearward flight. Below 40 knots airspeed, the center of gravity shift results in merely a change in down flapping away from the center of gravity for all airspeeds. In this low-speed regime, the principal effect of center of gravity location is on the fuselage attitude.

Above about 40 knots, the aerodynamic effects of the center of gravity on pitch stability become important. Increased pitch stability at forward cg tends to make the fuselage resist following the rotor in the down forward flapping necessary to tilt the thrust vector forward for high speed flight. At aft cg, the flapping remains relatively constant from 40 to 140 knots, reflecting both the reduced fuselage pitch stability and the more powerful effects of elevator gearing when the cyclic control is well forward, as required when flying at aft cg. The elevator gearing used in this ship is shown in Figure 11.

Lateral center of gravity offsets do not affect the pitch stability as do longitudinal cg effects, as shown in Figure 12. Thus, the effect in high speed flight is primarily a lateral flapping down and away from the cg location with very small changes in flapping trends with airspeed.

It should be noted that extreme right lateral cg locations in combination with forward cg locations will give large magnitudes of down aft and left flapping in rearward flight. In other steady flight regimes, the flapping would not be excessive unless the center of gravity limits were exceeded by a large margin.

3.2.3 Effect of Sideslip

Previous studies of flapping (unpublished Army data) have indicated that large sideslip angles can cause high flapping, which made this parameter variation of particular interest. The initial study, as presented in Figure 13, indicated that flapping was relatively insensitive to sideslip. The baseline utility helicopter was flown at 15-degree sideslip angles from -35 to 140 knots airspeed. Even at 140 knots, the change in flapping for a net change of 30° sideslip angle was less than 2°.

The fuselage was modified to include a large rolling moment due to sideslip term (dihedral effect) to show that this fuselage aerodynamic term was very important in describing flapping due to sideslip, as shown in Figure 14. Both positive

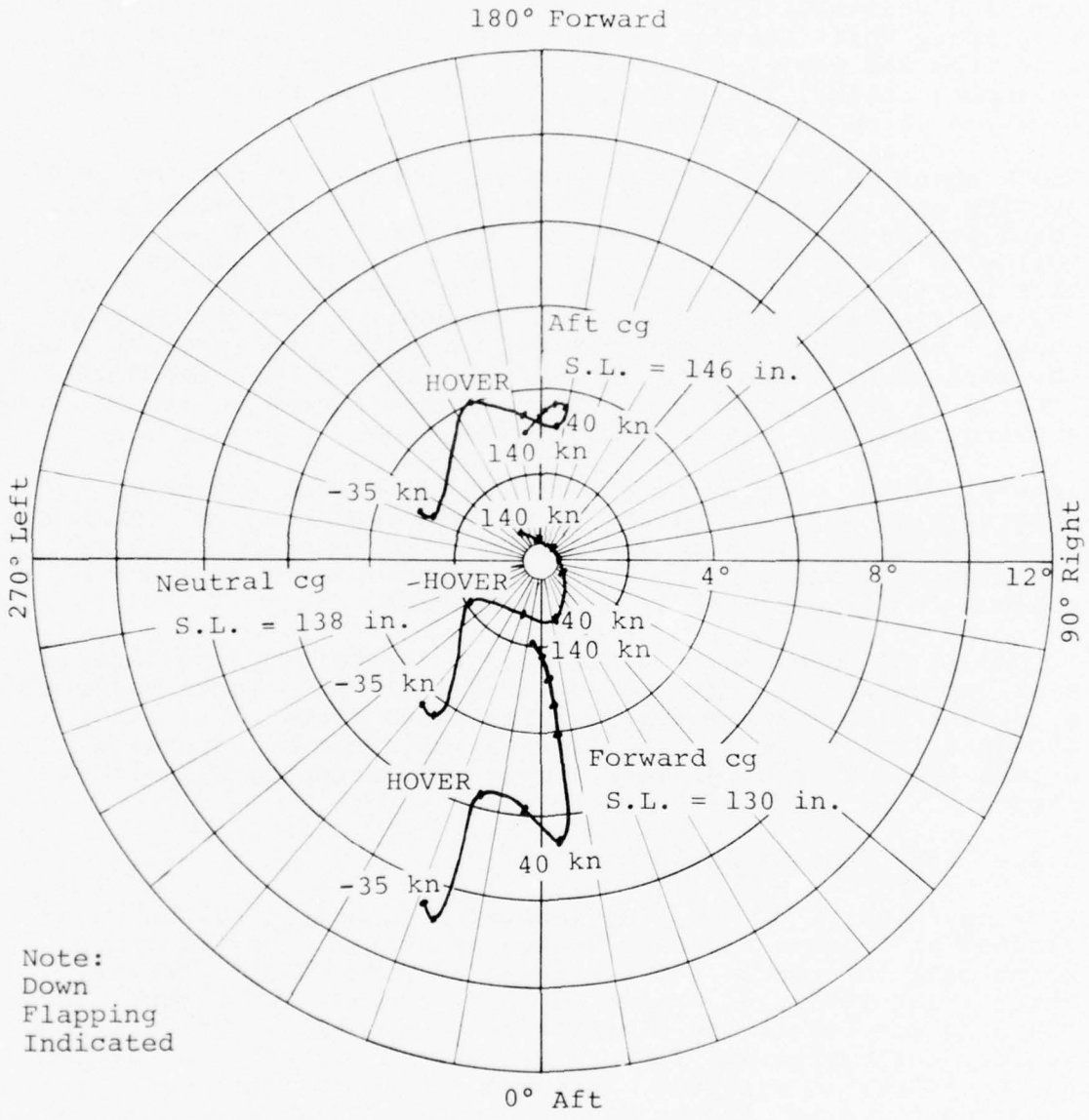

Figure 10. Effect of longitudinal center of gravity position on main rotor flapping in trimmed level flight.

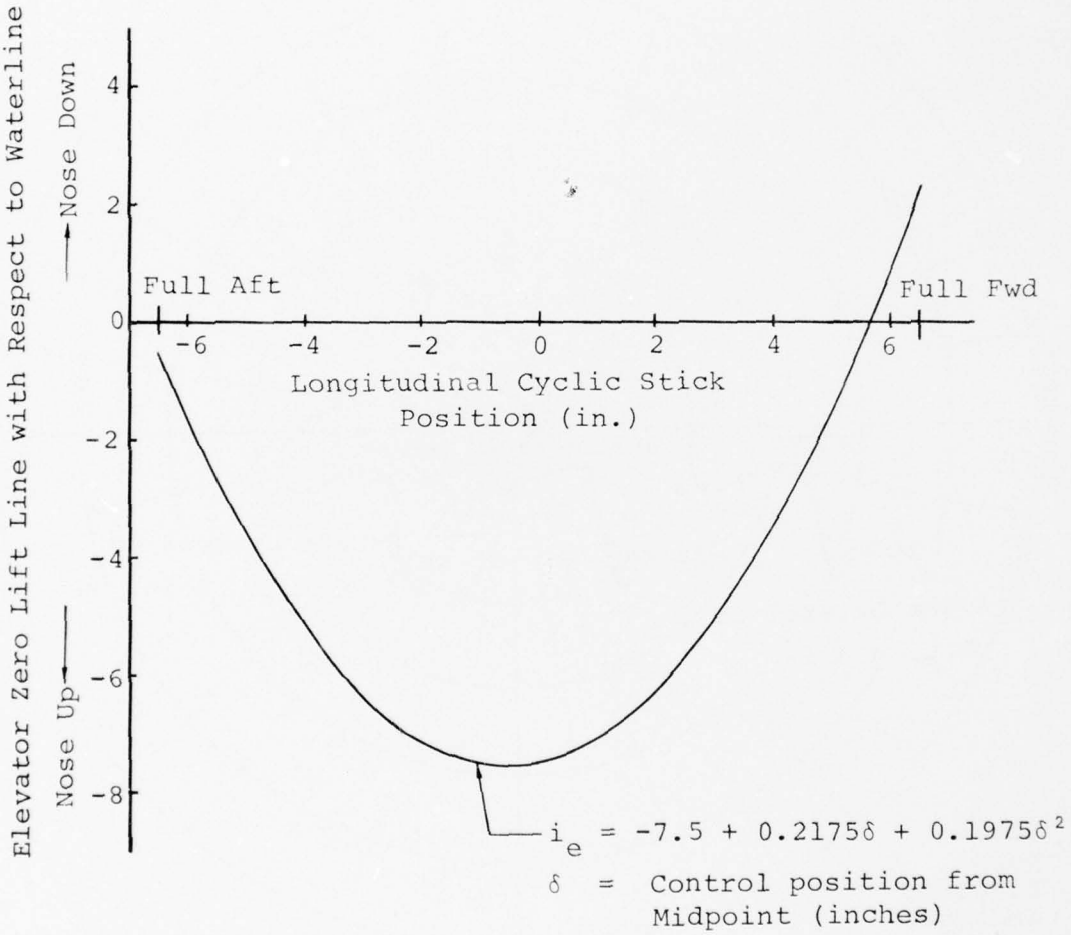

Figure 11. Elevator gearing used on the Utility Helicopter math model.

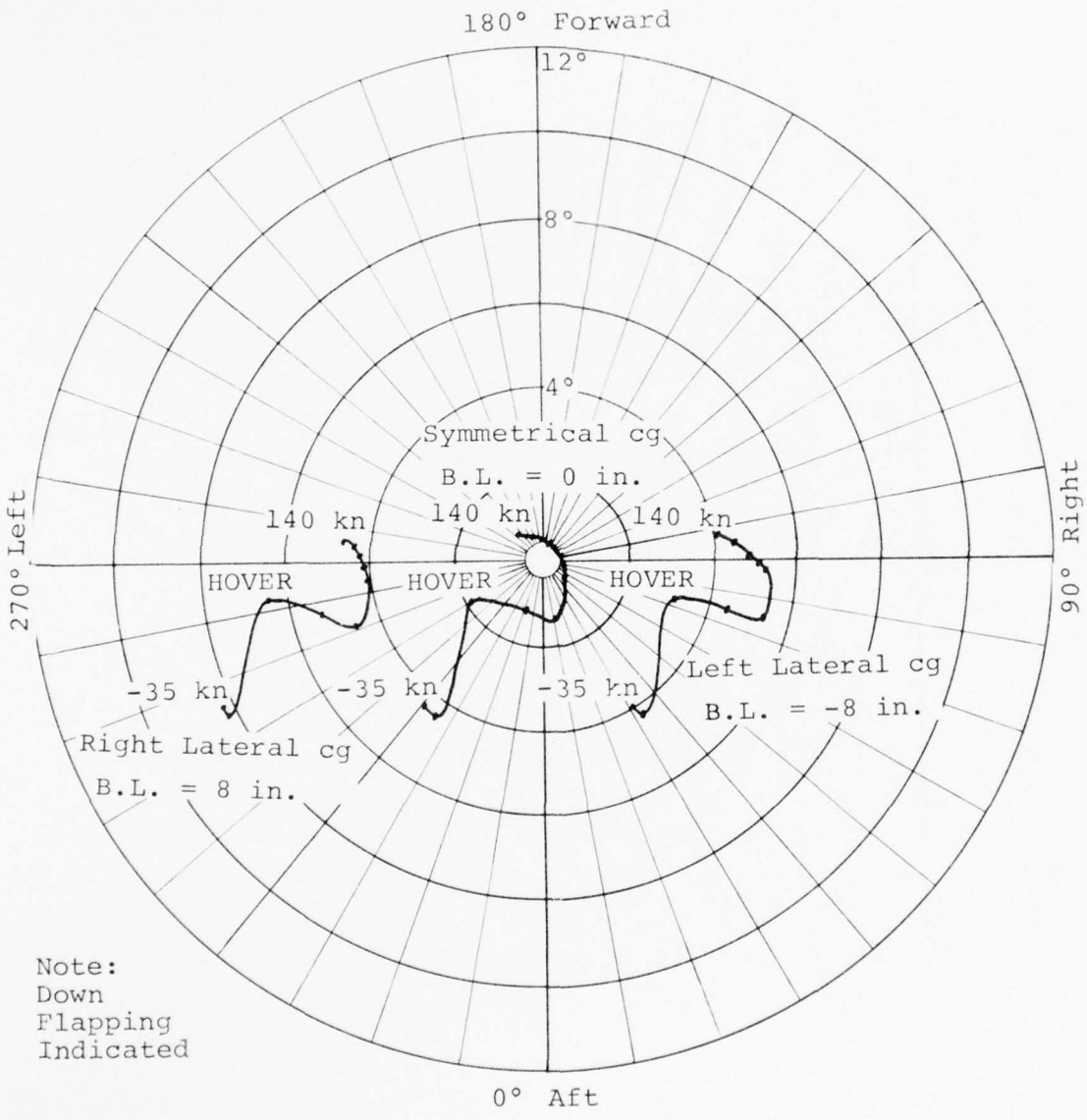

Figure 12. Effect of lateral center of gravity position on main rotor flapping in trimmed level flight.

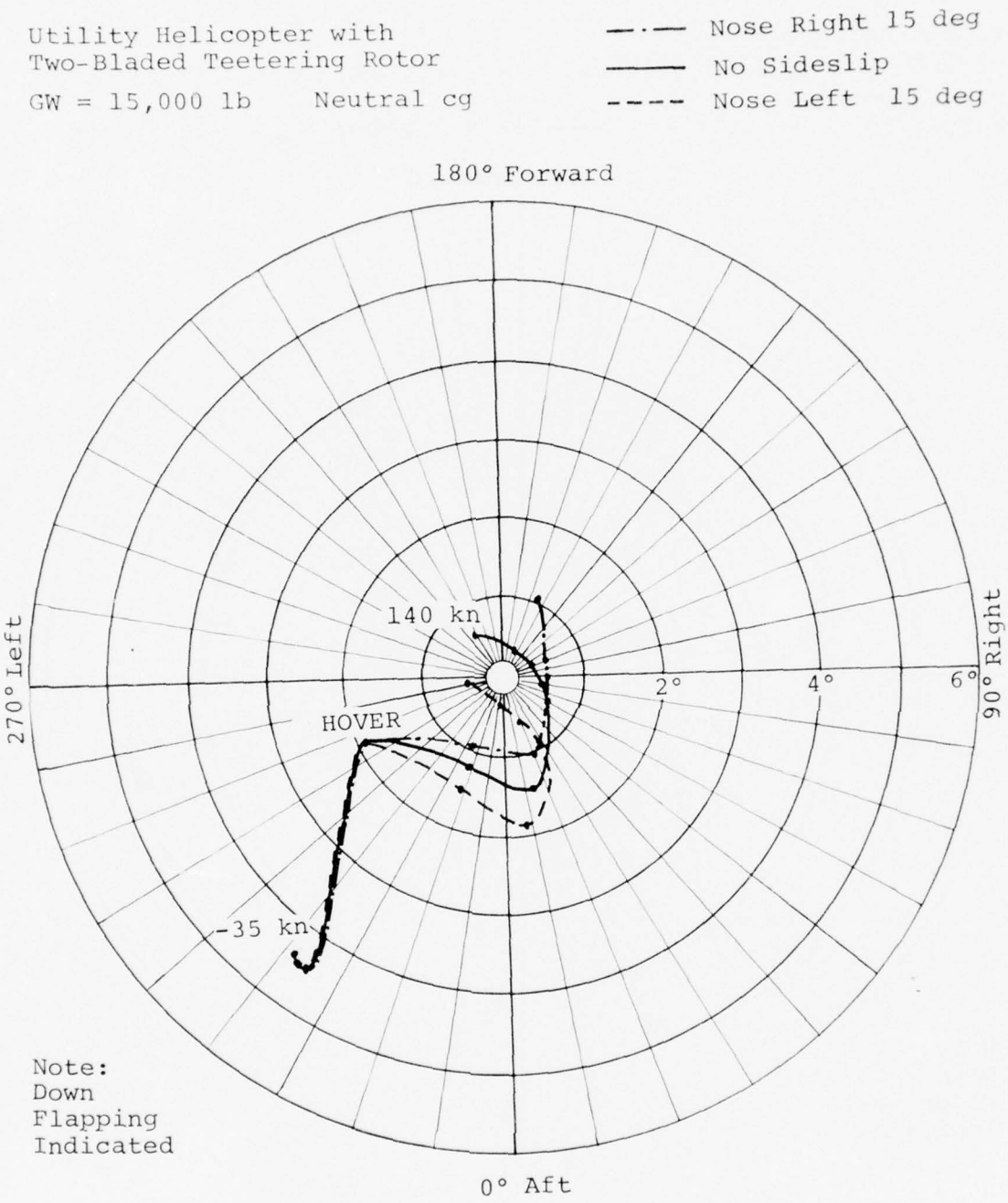

Figure 13. Effect of sideslip on main rotor flapping in trimmed level flight.

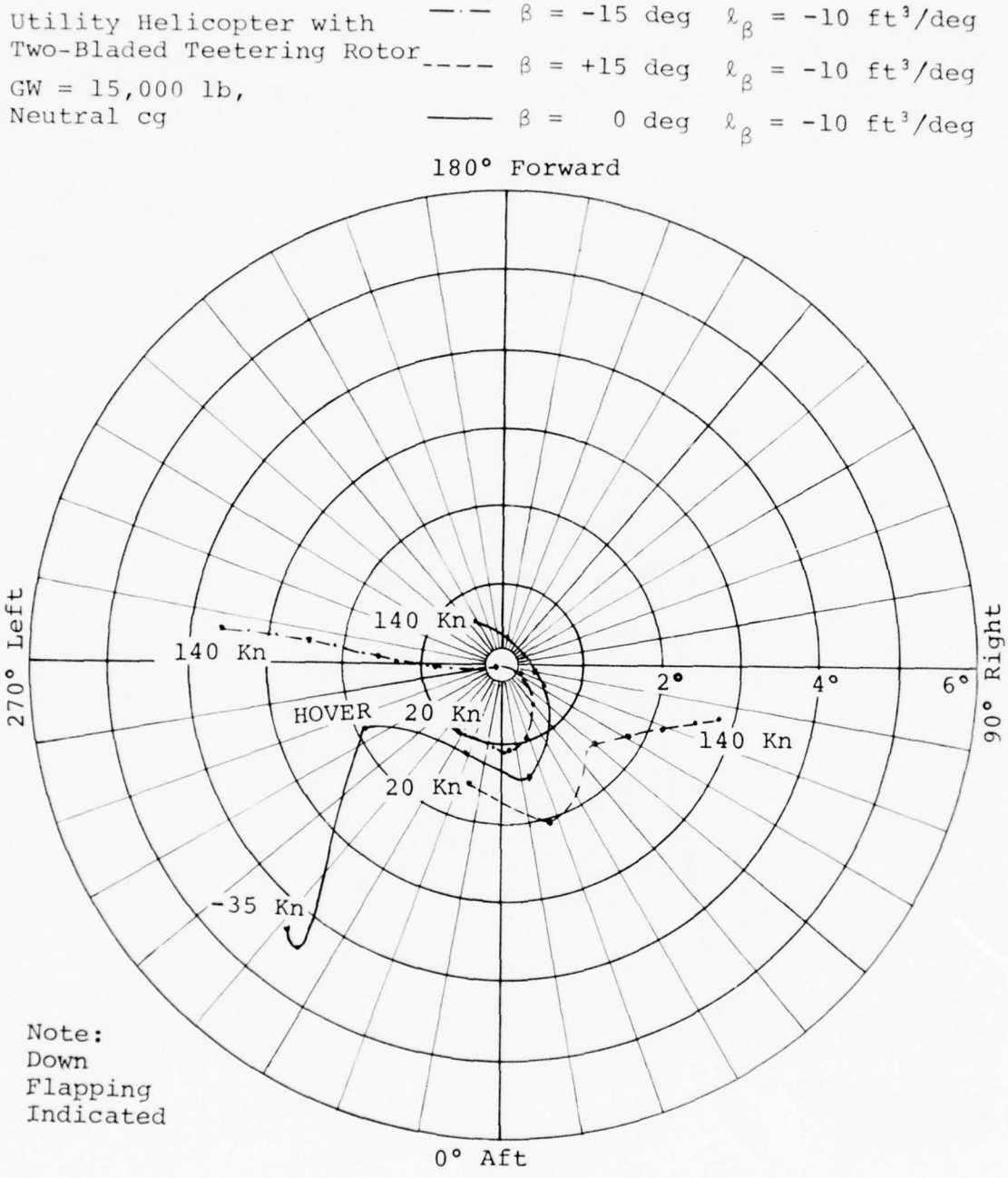

Figure 14. Effect of dihedral on main rotor flapping in trimmed sideslip level flight.

(right rolling moment due to nose right sideslip) and negative dihedral effect caused significant changes in flapping. The magnitude of fuselage dihedral was exaggerated for this study but the trend was unmistakable: the effective dihedral stability of the fuselage was the driving factor in steady-state sideslip flight.

It should be noted that excessive positive or negative dihedral would not be acceptable from a handling qualities standpoint and that this steady flight effect would not be likely on production aircraft.

The previous studies indicated that high flapping was measured in flight test in right sideward flight, while left sideward flight gave lower flapping. This led the researchers to the conclusion that nose left sideslip would cause large flapping in high-speed forward flight. The data obtained in the present work contradict this conclusion and led to a study of the reasons large flapping angles were measured.

The data source used by these researchers that gives the high flapping in right sideward flight was available, and the loading condition for this test was found to be maximum forward cg for the test aircraft. In this condition, the flapping in hover was almost 4-1/2° and would be down aft for the forward cg loading. The maximum flapping in left sideward flight was 4-1/4° and, in right sideward, was slightly over 9°. In rearward flight, 7-3/4° flapping was measured.

As noted in the discussion of sideward flight flapping characteristics, the low advance ratio inflow effect and the elevator download variation will produce down aft flapping for right sideward flight. When this effect is coupled with the down aft flapping due to the forward cg loading, significant flapping magnitudes will result.

It is concluded that the large flapping measured in right sideward flight was in the down aft direction and was caused by the low advance ratio effect and the loss of download on the elevator. While this is a real effect in the sideward flight environment, the extension of this tendency to higher speeds would be erroneous.

3.2.4 Effect of Gross Weight

For a given flight condition, an increase in gross weight will require a higher thrust level and, because of the increased torque needed, larger antitorque force.

Figure 15 illustrates the flapping trends of the baseline helicopter in forward and rearward flight with gross weights from 10,000 lb to 20,000 lb. At low speeds, more down left flapping occurs as gross weight increases, because of the left main rotor thrust tilt necessary to balance the increasing antitorque force. As forward speed increases, the lighter gross weight configuration requires more down forward flapping. Since the aerodynamic drag is about the same regardless of gross weight, the light-weight main rotor thrust vector must tilt further forward to provide the same propulsive component for a given airspeed. More thrust vector tilt requires more down flapping in the direction of the thrust vector.

3.2.5 Effect of Rotor RPM

Variation in rotor rpm is significant in high speed forward flight primarily because of its effect on retreating blade stall and on advancing blade Mach number (Figure 16).

At high airspeeds, if the rpm is too low, the retreating blade will enter a stall regime which causes down aft flapping. This stall becomes a significant factor at higher speeds and low rpm (high advance ratios) and will limit the maximum airspeed attainable.

At high rpm and high speed, the advancing blade reaches a Mach number above the drag divergence Mach number of the blade airfoil. The additional rotor drag requires more forward flapping to produce more propulsive force. At the highest speeds calculated, a large horsepower increase is required (at 140 knots, an increase from 300 to 330 rpm required an additional 1000 horsepower).

At low airspeeds, the main effect of rotor rpm is the change in tail rotor thrust requirements to compensate for main rotor torque changes with rpm. Increased tail rotor thrust requires a main rotor thrust component to the left, which will give down left flapping.

3.2.6 Effect of Fuselage Angle of Attack

The wide variation in fuselage angle of attack over the operating range of the helicopter was considered.

Climbs and descents are the most common sources of large, steady angle of attack changes seen by the helicopter. Climb and descent speeds of 600 and 1200 fpm were run over the forward speed range of 60 to 140 knots. The 1200 fpm data is presented in Figure 17. The major effect on flapping is the change in antitorque requirements, which requires down left flapping in climbs. A discontinuity is found between 60 and 80 knots in

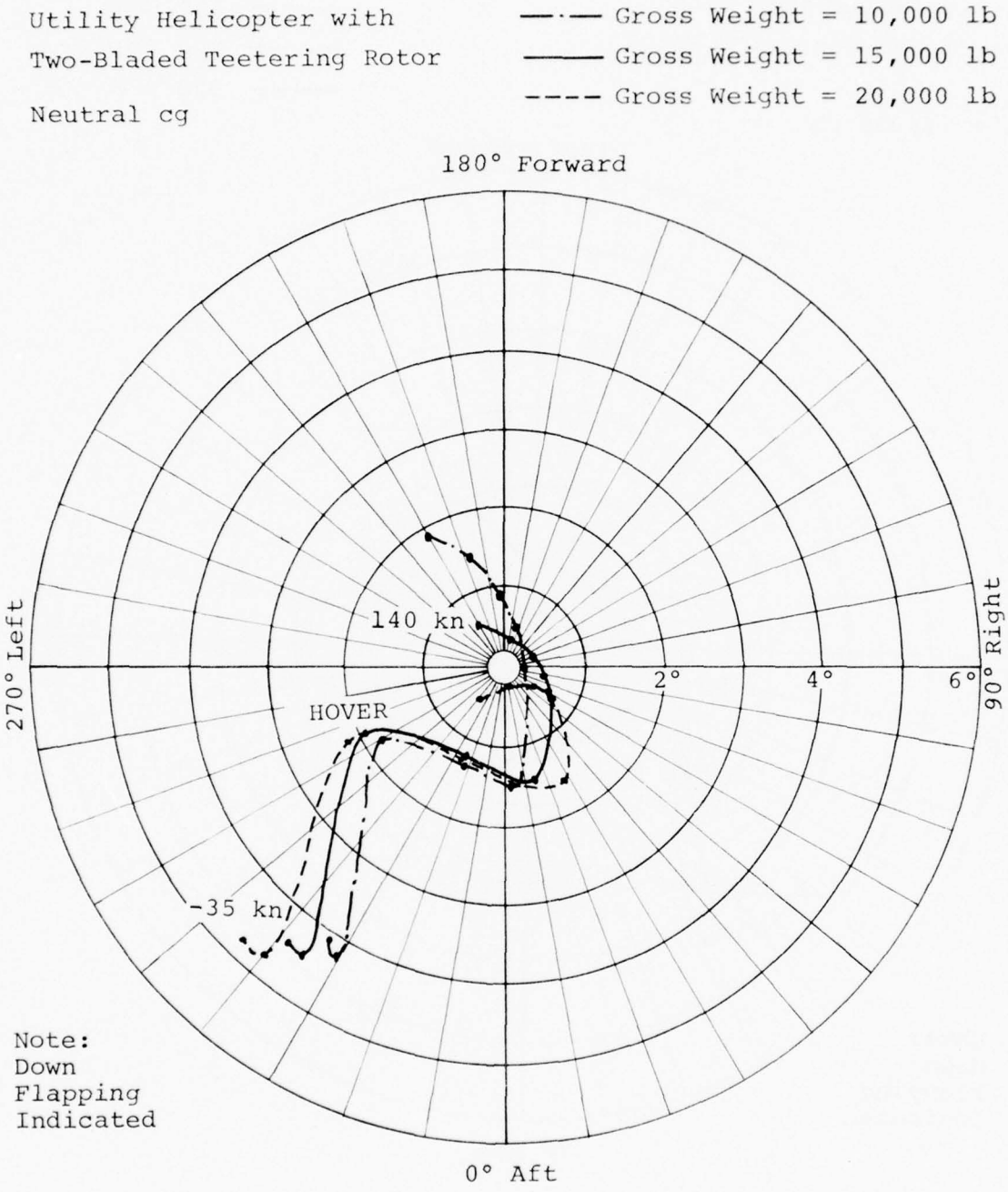

Figure 15. Effect of gross weight on main rotor flapping in trimmed level flight.

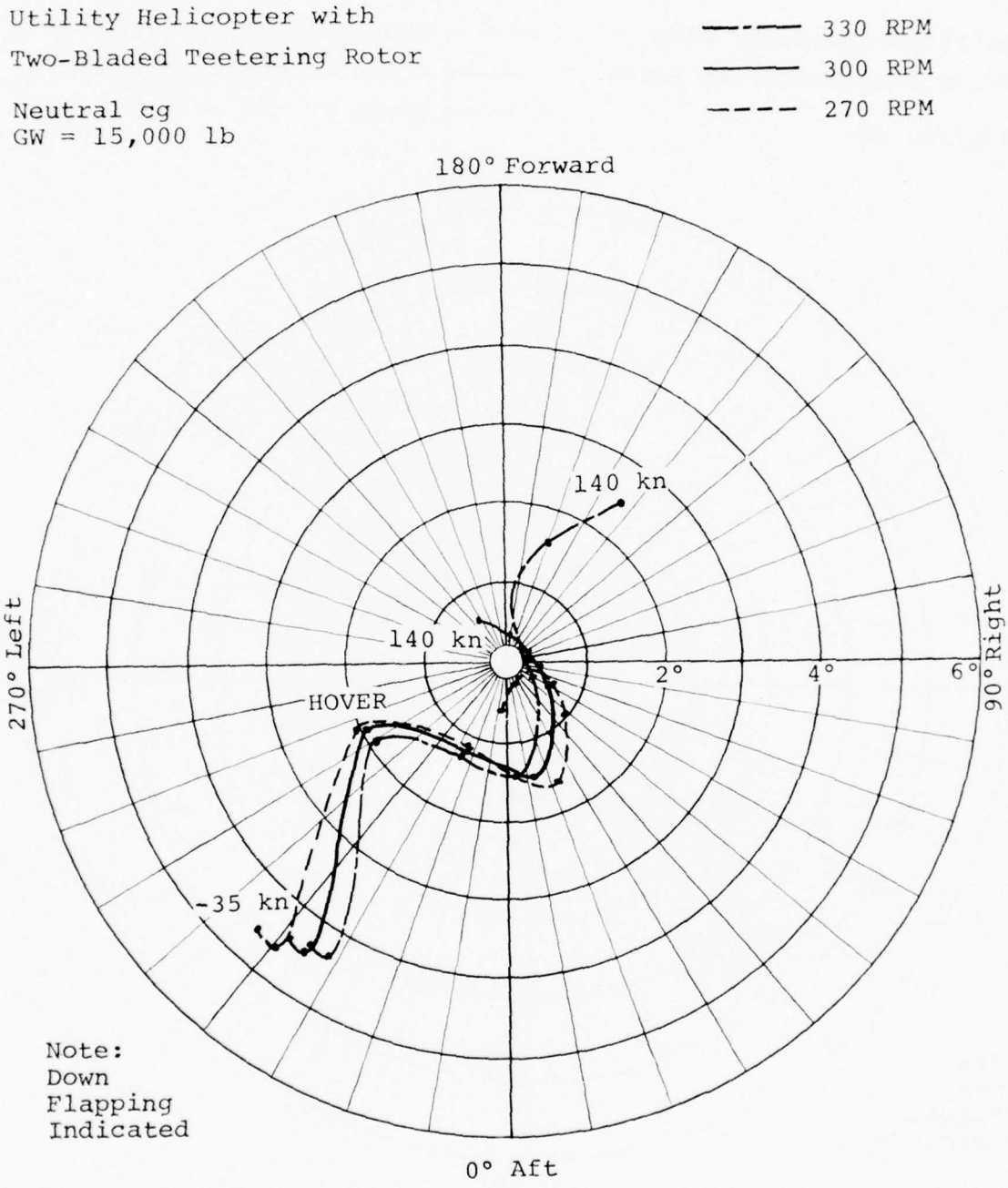

Figure 16. Effect of rotor RPM on main rotor flapping in trimmed level flight.

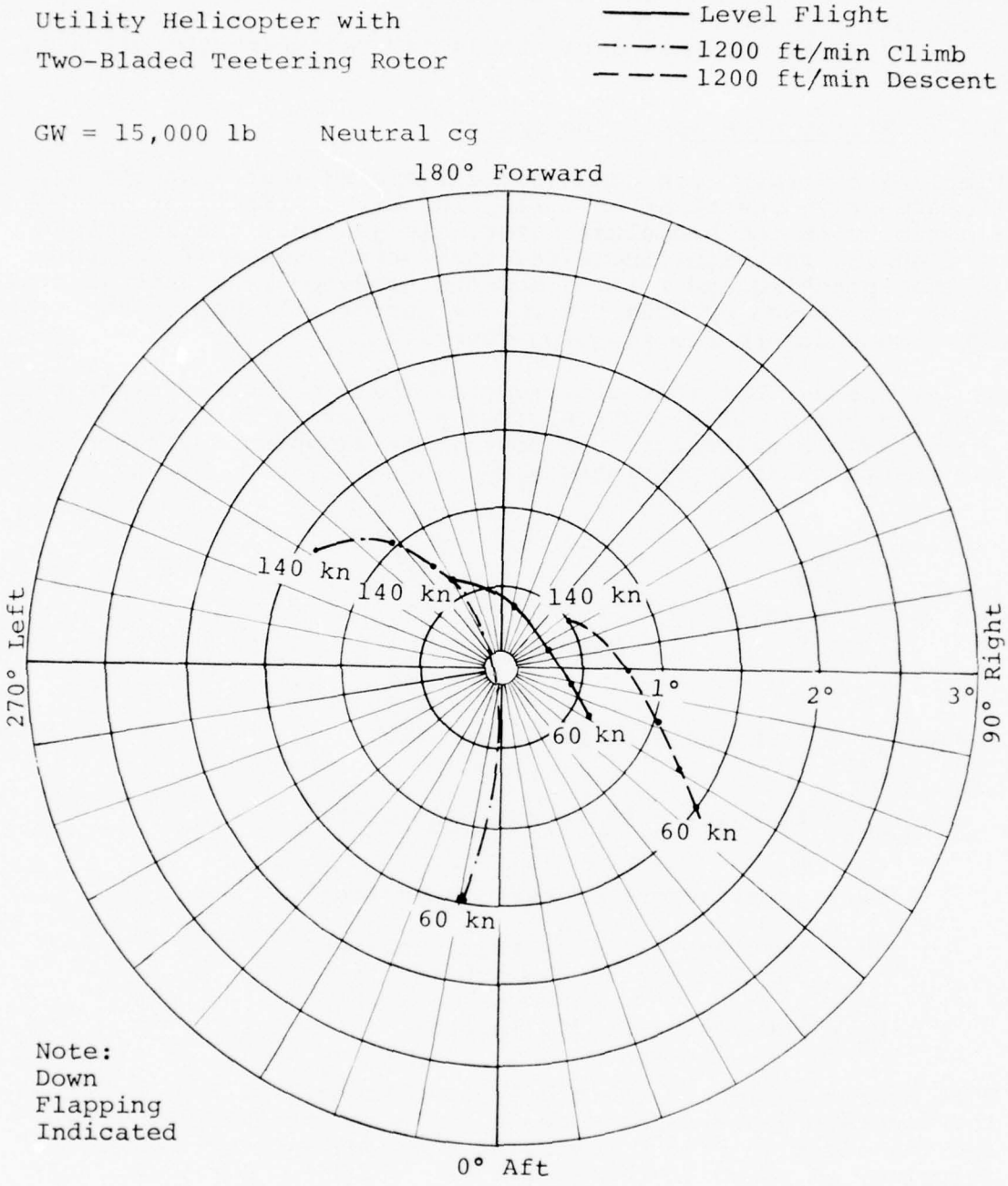

Figure 17. Effect of climbs and descents on main rotor flapping in trimmed flight.

climb due to stalling of the horizontal stabilizer. The math model has a sharp change in lift once stall is reached and, compared to flight test data, tends to exaggerate the pitching moment effect.

3.2.7 Effect of Flapping Restraint

Flapping restraint can come from a flapping restraint spring, the effective restraint of a flapping hinge offset, or the hub elasticity in the hingeless rotor. In general, the addition of flapping restraint increases the control power of the rotor in that pitching and rolling moments produced by a unit swashplate input are caused by both the thrust vector tilt and an additional hub moment due to the flapping restraint.

At low speeds, hub restraint reduces the angle between the rotor disk and the fuselage, which gives a reduction in flapping with increased hub restraint. In hover, the flapping variation with hub restraint is approximately:

$$\frac{\beta_{K_H}}{\beta_{K_H=0}} = \frac{1}{1 + \frac{K_H}{(GW)(h)}}$$

where β_{K_H} = flapping with hub restraint

$\beta_{K_H=0}$ = flapping with no hub restraint

GW = gross weight of helicopter (lb)

h = vertical distance from fuselage vertical cg to the hub (ft)

K_H = hub restraint (ft lb/rad)

This approximation is valid only near hover. At higher speeds, the fuselage aerodynamic moments dominate the flapping angle, and the addition of hub restraint makes only minor changes in flapping, as shown in Figure 18.

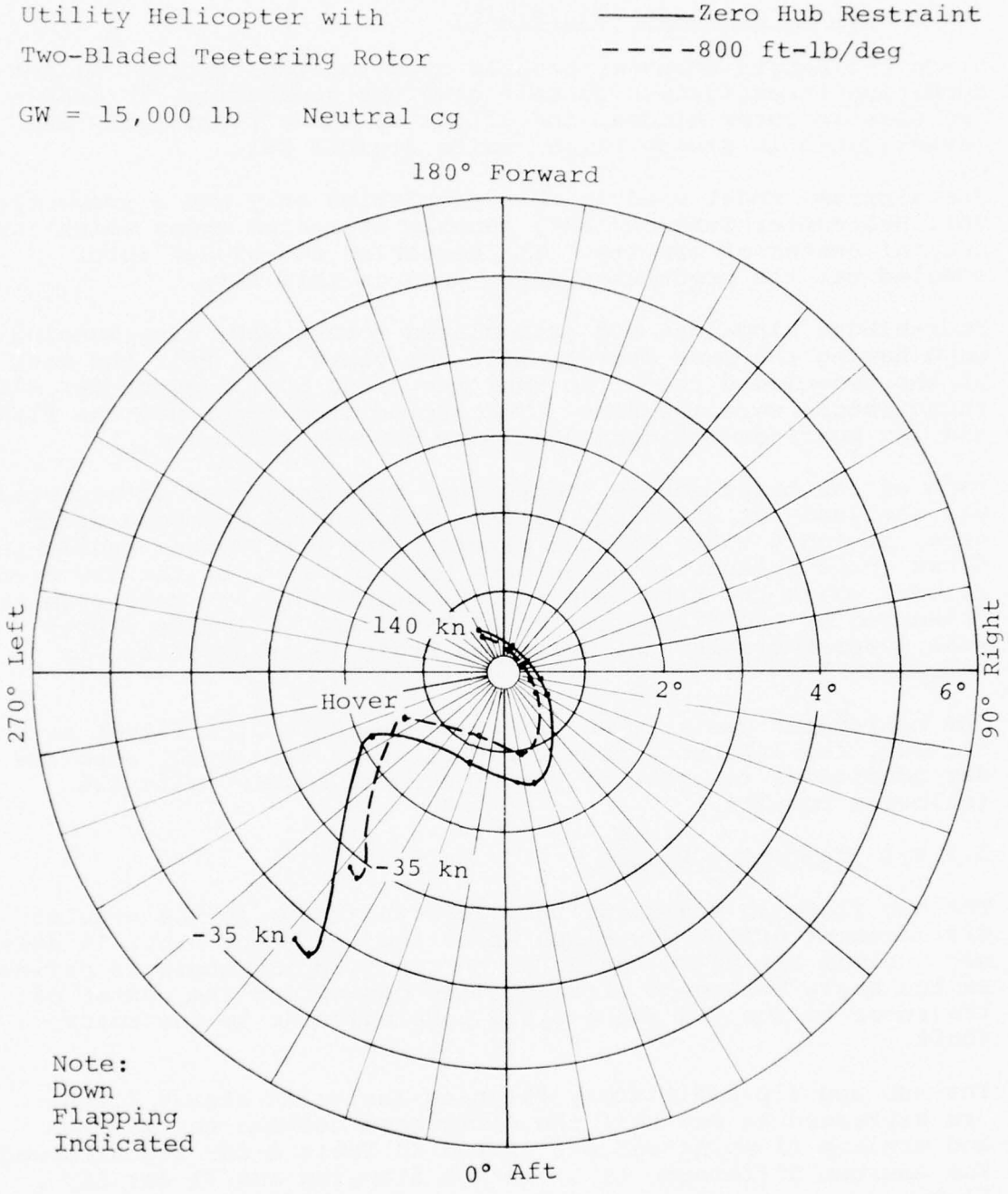

Figure 18. Effect of hub restraint on main rotor flapping in trimmed level flight.

3.2.8 Effect of Blade Flexibility

Since the hybrid computer program used for the critical flight condition investigation doesn't have the capability of modeling elastic rotor blades, the effect of blade flexibility was investigated in steady flight using digital C81.

The airframe model used in this simulation only was a production Bell Helicopter Textron (BHT) gunship at medium gross weight and neutral center of gravity. The teetering two-bladed rotor modeled was the production rotor used on this ship.

Four-bladed hingeless and articulated rotors were also modeled, each having the same radius, half the chord, and half the mass of the two-bladed rotor, so that the blade Lock numbers for all three rotors were the same. The articulated rotor had the flap and lag bearings collocated at five percent radius.

Each of the basic rotors (teetering, hingeless, and articulated) was analyzed for standard, halved, and doubled beamwise stiffness, giving a total of nine rotors. The first three cyclic and first three collective modes were used for each of the teetering rotors, while the hingeless and articulated rotors were each represented by the first four scissors modes. All mode shapes were generated using the Myklestad Analysis as described in Reference 12.

The helicopter was trimmed in level, unaccelerated flight at 60, 100, and 140 knots true airspeed under sea level, standard day conditions for each of the nine rotor models, with the follcwing results:

3.2.8.1 Teetering Rotors

The hub flapping angle for the teetering rotor is the angular displacement of the rigid hub about the teetering pin. It does not include any blade coning. The tip flapping angle is defined as the angle between a straight line connecting the center of the rotor to the tip and a plane perpendicular to the rotor shaft.

The hub and tip oscillatory flapping angles in steady flight are expressed as one-half the difference between the maximum and minimum flapping and are listed in Table 3 for two airspeeds. The maximum difference of 6% in hub flapping and 7% for tip flapping is given for a change in blade stiffness by a factor of two.

---

[12] R. L. Bennett, DIGITAL COMPUTER PROGRAM DF1758: FULLY COUPLED NATURAL FREQUENCIES AND MODE SHAPES OF A HELICOPTER ROTOR BLADE, Report No. 299-099-724, Bell Helicopter Textron, Fort Worth, Texas, March 1975.

TABLE 3. EFFECT OF BLADE FLEXIBILITY ON AMPLITUDE OF TIP FLAPPING ANGLE FOR TEETERING ROTOR

Airspeed	Flapping Amplitude[1]		
	Baseline Blade Stiffness	½ x Baseline Blade Stiffness	2 x Baseline Blade Stiffness
60 Kn	1.717 deg	1.729 deg	1.706 deg
100 Kn	0.467 deg	0.453 deg	0.467 deg
140 Kn	2.300 deg	2.323 deg	2.368 deg

[1]Flapping amplitude given as ½ peak-to-peak value in degrees.

3.2.8.2 Articulated Rotors

The flapping angles for the articulated rotor are the angles formed between the plane perpendicular to the shaft and a reference line. For the root flapping, the reference line is a straight line from the flapping hinge, at five percent radius, and a point on the blade at ten percent radius, while for the tip flapping, the reference line is a straight line connecting the center of the rotor and the tip. The hub and tip flapping angles are presented in Table 4. Only the root flapping at 140 knots shows any appreciable change due to change in the blade beam stiffness, with the 1/2 peak-to-peak amplitude root flapping of the stiffer blade being greater than that of the soft blade. This is to be expected since the increased stiffness will tend to make the root flapping approach the magnitude of the tip flapping.

3.2.8.3 Hingeless Rotors

The flapping angles for these rotors are the angles between the plane perpendicular to the shaft and a straight line connecting the center of the rotor to a reference point on the blade. For the root flapping, this reference point is at five percent radius, while the tip flapping uses the tip for the reference point. Table 5 gives the oscillatory variation of these angles for the three rotors at 60- and 140-knot steady level flight. The stiffer blade generally has less root and tip flapping than the baseline blade, while the softer blade has more root flapping at both airspeeds and generally higher tip flapping for the high-speed case. Again, the differences are small for factor-of-two changes in the beam stiffness.

Blade stiffness is seen to have only a minor effect on level flight main rotor blade flapping for the three rotor types investigated.

3.2.9 Gust Penetration

The analysis of rotor gust penetration is complicated by several factors. In the simplest case, that of a sudden gust (in which the additional inflow due to the gust is applied over the entire rotor disk instantaneously), the analysis is complicated by determining the manner in which the lift builds up or decays. Also, the blade azimuth at the time of gust application must be considered. In this case, the maximum response occurs immediately after the gust application, and the fuselage response

TABLE 4. EFFECT OF BLADE FLEXIBILITY ON AMPLITUDE OF HUB AND TIP FLAPPING ANGLES FOR ARTICULATED ROTOR

Airspeed and Flapping Location	Flapping Amplitude[1]		
	Baseline Blade Stiffness	½ x Baseline Blade Stiffness	2 x Baseline Blade Stiffness
60 Kn, HUB	0.391 deg	0.365 deg	0.365 deg
60 Kn, TIP	0.349 deg	0.348 deg	0.331 deg
140 Kn, HUB	0.469 deg	0.443 deg	0.573 deg
140 Kn, TIP	0.697 deg	0.692 deg	0.681 deg

[1]Flapping amplitude given as ½ peak-to-peak value in degrees.

TABLE 5. EFFECT OF BLADE FLEXIBILITY ON AMPLITUDE OF ROOT AND TIP FLAPPING ANGLES FOR HINGELESS ROTOR

Airspeed and Flapping Location	Flapping Amplitude[1]		
	Baseline Blade Stiffness	½ x Baseline Blade Stiffness	2 x Baseline Blade Stiffness
60 Kn, ROOT	0.130 deg	0.157 deg	0.078 deg
60 Kn, TIP	0.296 deg	0.318 deg	0.256 deg
140 Kn, ROOT	0.156 deg	0.183 deg	0.208 deg
140 Kn, TIP	0.657 deg	0.721 deg	0.619 deg

[1]Flapping Amplitude given as ½ peak-to-peak value in degrees.

can be neglected in the analysis, but even with this simplification, there is no simple analysis available. Furthermore, the sudden gust is not a realistic loading condition, and analysis of gradual gust penetration (in which the gust velocity builds up over a certain distance and is not applied to the whole disc simultaneously) is a more complicated problem. Due to the lack of any simplified gust analysis, digital C81 was used to determine the flapping response of teetering, hingeless and articulated rotors upon gust penetration.

In this study, the fuselage was the Bell Helicopter Textron production gunship used in the blade flexibility study. The rotors modeled were: the teetering rotor modeled by the first cyclic and first collective modes; the hingeless rotor modeled by the first scissor mode; and the articulated rotor modeled by the first two scissor modes (rigid body flapping and rigid body lead-lag mode).

The C81 model of each of the three rotor types of the helicopter was "flown," stick-fixed, through ten different vertical sine-squared gusts at two different airspeeds, for a total of 20 gust penetrations per rotor type.

The gust lengths and maximum velocities, chosen as representative of the distribution given in Reference 13, are listed in Table 6.

For all rotors at both airspeeds, Gust D produced the largest flapping excursions from trim. The rotor flapping peaks followed the general trend of lower peaks for high-effective hub restraint and higher peaks for higher airspeeds, as given in Table 7.

---

[13] K. W. Harvey, B. L. Blankenship, and J. M. Drees, ANALYTICAL STUDY OF HELICOPTER GUST RESPONSE AT HIGH FORWARD SPEEDS, USAAVLABS Technical Report 69-1, U.S. Army Aviation Materiel Laboratories, Fort Eustis, Virginia, Sep. 1969, AD 862594.

TABLE 6. GUST CHARACTERISTICS FOR SIMULATIONS

Gust	Gust Length (feet)	Maximum Gust Velocity (ft/sec)
A	80	±30
B	180	±10
C	180	±30
D	180	±50
E	360	±30

TABLE 7. FLAPPING EXCURSIONS DUE TO GUSTS

Rotor Type	Airspeed (kn)	Δ Max Flap @ Hub/Gust Type	Δ Min Flap @ Hub/Gust Type	Δ Max Flap @ Tip/Gust Type	Δ Min Flap @ Tip/Gust Type
Teetering	60	2.18°/D up	-	3.57°/D up	-1.89°/D down
Teetering	140	3.04°/D up	-	3.80°/D up	-3.42°/D down
Articulated	60	2.65°/D up	-1.73°/D down	2.59°/D up	-1.69°/D down
Articulated	140	2.93°/D up	-2.85°/D down	2.85°/D up	-2.78°/D down
Hingeless	60	0.94°/D up	-0.66°/D down	2.40°/D up	-1.70°/D down
Hingeless	140	1.16°/D up	-1.23°/D down	2.97°/D up	-3.12°/D down

NOTE: ΔMax Flapping = Max Flapping Peak After Gust - Max Flapping Peak Before Gust

ΔMin Flapping = Min Flapping Peak After Gust - Min Flapping Peak Before Gust

4. PILOT LIMITS

In order to perform the critical flight maneuver simulation, a clear picture of likely pilot actions is required. Possible pilot inputs will be governed by how fast he can move the controls, what parameters will stimulate his response, and to what level he will accept these stimuli before reacting. With this information, a reasonable pilot model may be obtained to govern the maneuvers to be performed.

4.1 CONTROL MOVEMENT LIMITS

The first of these items, how fast the pilot is able to move the controls, is readily available through results presented in Reference 14. The speed with which the controls may be moved is a function of the distance moved, the force required, the precision required, and the type of movement. In terms of control movements which could lead to high flapping situations, we are primarily concerned with how fast a large input can be made in the cyclic control system. For example, from the middle of a large cyclic stick range, a rapid movement to the stick stop could be made in about 0.3 seconds for a 7-inch motion. From stop to stop, about 0.37 seconds will be required to travel 13 inches. This assumes ideal conditions with less than 2 pounds of force required and no reaction time. However, typical cyclic control boost cylinders are rate-limited to between 0.5 seconds (no load) and 1.0 seconds for full travel. Obviously, even with a large cyclic stick travel, the pilot can move faster than the boost system and will be thus limited to no less than 0.5 seconds for a full-throw motion of the cyclic stick. This was the pilot cyclic control rate limit used for this study - full-throw in 0.5 seconds.

The most difficult task in establishing a pilot model is to define and record the stimuli that generate pilot action. Examples are fuselage attitudes, rates and accelerations, vibration levels, normal load factor, instrument readings, or noise levels. Out of all the possibilities, only fuselage rates and attitudes and normal load factors could be interpreted with confidence from the hybrid computer simulation.

---

[14]A. Damon, H. W. Stoudt, and R. A. McFarland, THE HUMAN BODY IN EQUIPMENT DESIGN, Cambridge, Mass., Harvard University Press, 1966.

4.2 FUSELAGE RATE AND ATTITUDE LIMITS

The magnitude of these fuselage parameters that a pilot will tolerate is the next problem of simulation. Since motion about more than one axis is possible at any time, the tolerance level for allowable attitudes and rates becomes very difficult to establish. Helicopter structural demonstrations, which involve maximum load maneuvers, have used fuselage rate and attitude limitations based on test pilot experience.

Table 8 presents these fuselage rate and attitude limits, which are used as guidelines for establishing the severity of a maneuver. Two sets of conditions are established in this table. The absolute limits are values of attitudes or rates that, when encountered, will simply cause pilot action to reduce the value. When both rates and attitudes are considered in combination, the tolerable levels are decreased substantially, as seen in the column marked combination. No attempt was made to establish tolerable limits for rates and attitudes in combination about more than one axis.

When the fuselage rate or attitude limits of Table 8 were reached during a simulated maneuver, the maneuver was considered severe enough to expect the pilot to attempt recovery.

TABLE 8. FUSELAGE RATE AND ATTITUDE LIMITS

Fuselage	Absolute Limits	Combination Limits
Pitch Angle	±50 deg	+20 deg with +15 deg/sec; -20 deg with -10 deg/sec
Pitch Rate	±20 deg/sec	
Roll Angle	±70 deg	±55 deg with ±25 deg/sec
Roll Rate	±60 deg/sec	
Yaw Rate	±55 deg/sec Hover ±15 deg/sec Forward Flight	

5. SIMULATION OF CRITICAL FLIGHT CONDITIONS

Flight experience has indicated several maneuvers that resulted in high main rotor flapping. The following flight conditions, which are representative of these maneuvers, were simulated using hybrid C81:

Roller-coaster maneuver (a rapid pull-up followed by a push-over at high airspeed)

Roll reversal maneuver (a large rapid lateral cyclic input followed by an opposite lateral input)

Autorotation entry (loss of engine power followed by a 2-second delay for a collective pitch reduction and flare)

Tail rotor loss (loss of tail rotor thrust and the weight of the tail rotor gearbox and blades followed by an autorotational entry)

Flares (constant altitude deceleration from 100 kn to hover and 60 kn flare to landing from steady autorotation)

Hard landings (landings at forward and aft cg extremes from 10-foot skid height hover with SCAS ON and OFF).

Jump take-off (collective pull to 1.75g vertical take-off at cg extremes)

Pop-up (collective pull to 1.5 g vertical climb from hover)

The first three maneuvers (roller-coaster, roll reversal, and autorotational entry) were run for all helicopter and rotor configurations for comparison of helicopter characteristics. These maneuvers involve most of the important parameters identified during the parametric investigation and are considered sufficient to identify critical flapping differences between rotor and helicopter types. The rest of the maneuvers were investigated using only the utility helicopter with a two-bladed teetering rotor.

5.1 ROLLER COASTER MANEUVER

This maneuver was a high speed (140 knots) cyclic pull-up to approximately $\approx$1.80 g followed by a cyclic pushover to a near zero (less than 0.1 g) g level and recovery to approximately level flight. This maneuver gave a good illustration of both high- and low-g effects. A typical time history of such a maneuver is shown in Figure 19.

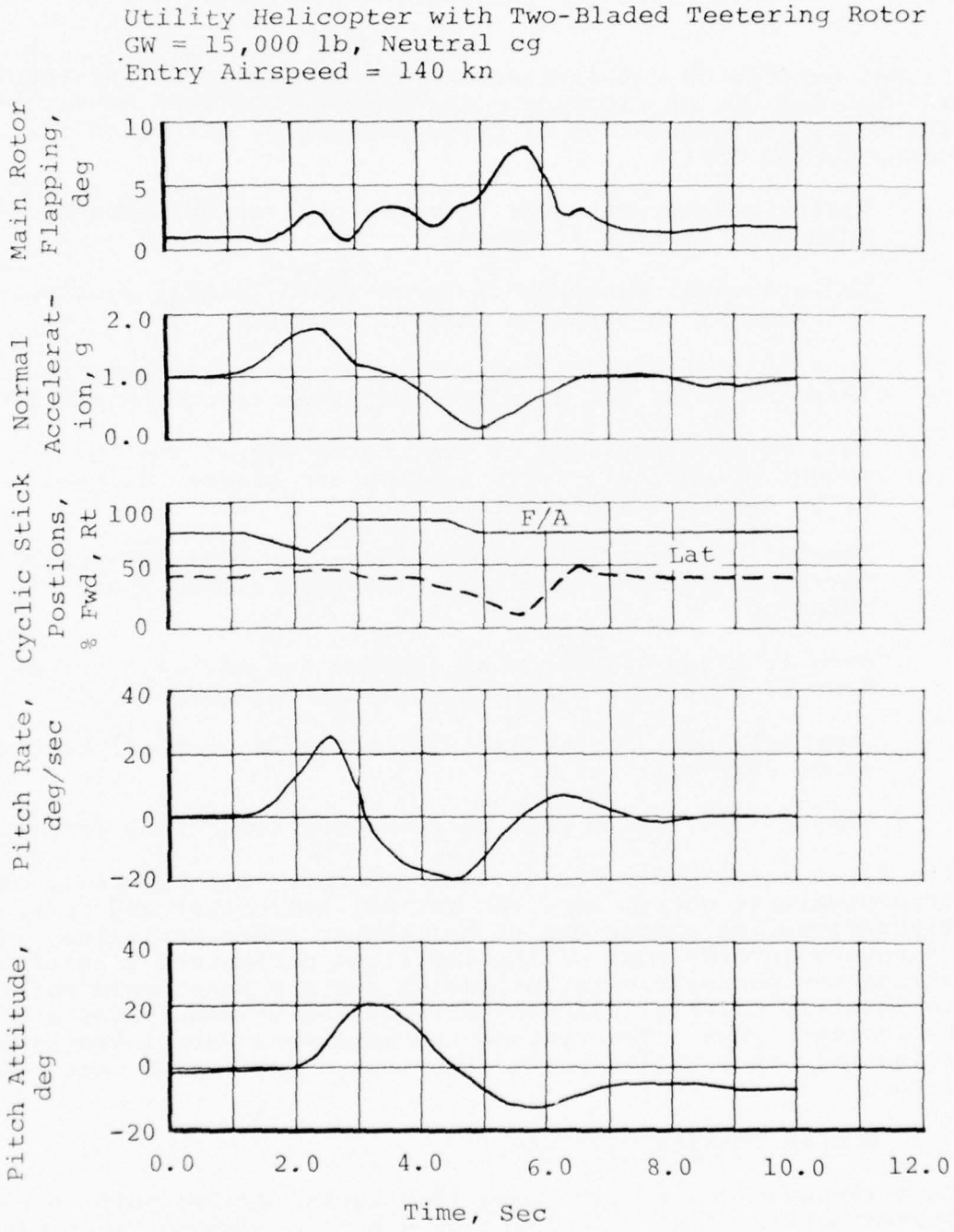

Figure 19. Typical roller-coaster maneuver.

To compare the same maneuver for all the helicopters, a standard longitudinal cyclic stick input was used. The time points for control movements were held constant for all helicopters, while the magnitude was adjusted to attain the desired g-levels.

Initial maneuvers were run with the rotor rpm fixed, which simulated a very "tight" engine governor. Later, an engine governor model was activated to simulate a typical governor, and the flapping peaks increased slightly. This maneuver was distinctly divided into the high- and low-g regimes, with different characteristics for each regime.

5.1.1 High-g Segment

In general, two flapping peaks were noted during the high-g segment of this maneuver. The first peak was a direct result of the aft cyclic stick input required to attain the g-level desired. This flapping peak was predominantly in the down aft (positive a_{1_s}) direction and was generally proportional to the magnitude of the initial control inputs. It should be noted that the controllable elevator will provide significant pitching moments at high speeds and that control coupling will also introduce some lateral flapping that will modify this initial flapping peak.

The second flapping peak occurred when the cyclic stick was moved forward to stop the nose-up pitch rate and start toward the low-g portion of the maneuver. This peak was a strong function of the lift capability of the retreating blade. The forward cyclic swashplate motion increases blade pitch at the $\psi = 270°$ azimuth, which, if the blade is close to stall, can initiate blade stall and give a down aft flapping tendency that will continue until the cyclic stick is moved aft to control the low-g portion of the maneuver. The action of the rotor in this type of maneuver is strongly dependent on the aerodynamic characteristics of the rotor near stall. These characteristics, while modeled mathematically, should be interpreted as a tendency for flapping, but the absolute value of flapping obtained may be questionable.

5.1.2 Low-g Segment

In order to attain the low-g portion of this maneuver, a nose-down pitch rate was generated with a forward cyclic stick input. The normal rotor coupling provides down right flapping with a nose-down pitch rate. In addition, as the rotor thrust decreases, the left thrust, which was counteracting the tail rotor thrust, is also reduced. These factors both contribute

to a right rolling moment and down right flapping. An additional factor that complicates the situation is the effect of negative roll damping due to a combination of large inflow velocity and low rotor thrust, as is documented in Reference 9.

The net result is a strong tendency for the helicopter to roll right with some down right flapping. In the computer simulation, the pilot model, reacting in the same manner as a pilot unaware of the proper recovery technique (apply aft cyclic stick to increase g-level), applied left lateral cyclic in order to stop the right roll. With little or no thrust available to produce a rolling moment with the teetering rotor system, large left flapping magnitudes were seen as a result of large left lateral cyclic swashplate inputs and right roll rate. With the addition of hub restraint, a rolling moment was available, and much less lateral cyclic input was required to maintain roll control. Consequently, the low-g flapping was reduced since most of the flapping seen in this peak was lateral. When aft cyclic stick is applied, thrust builds up, and the lateral flapping is reduced as the g-level increases.

5.1.3 Effect of cg Location and Gross Weight

Table 9 summarizes the flapping peaks during the roller coaster maneuver for the utility helicopter with a two-bladed teetering rotor as a function of the center of gravity location and gross weight.

The forward center of gravity location is seen to give the largest flapping in the high-g portion of the maneuver for two reasons.

First, when the helicopter is in trimmed flight at forward cg, the flapping will be predominantly down aft. The initial aft cyclic control input imposes more aft flapping, which is additive to the trim value. Conversely, at aft cg, the trim flapping is down forward, and when the aft cyclic is applied, the flapping must undergo a phase shift that will reduce the absolute magnitude of the flapping.

Second, the helicopter is statically more stable in pitch at forward cg and will require more pitching moment to be applied to attain the pitch rates necessary to attain a given g level. This will require larger magnitude longitudinal control inputs. Another factor in supplying this pitching moment is a movable horizontal stabilizer. The elevator gearing curve for the UH aircraft is shown in Figure 11. The cyclic stick position required for trim moves forward as the cg moves aft. A change of one inch of longitudinal cyclic stick would give a larger increment of elevator incidence at aft cg than at forward cg with a resultant larger pitching moment increment. This decreases the amount of pitching moment to be supplied by the rotor and decreases the rotor flapping.

TABLE 9. GROSS WEIGHT AND CG EFFECTS ON FLAPPING IN THE ROLLER-COASTER MANEUVER

Utility Helicopter, Two-Bladed Teetering Rotor, No Hub Restraint

Gross Weight (lb)	cg Location (in)	Flapping Peaks[1] Trim (deg)	Initial (deg)	Second (deg)	Low g (deg)	Max. Load Factor (g)	Min. Load Factor (g)
15,000	138	1.2 F	3.0 A	5.9 A	10.8 F/L	1.80	0.12
15,000	130	1.7 A/L	8.4 A	9.7 A	8.9 L	1.85	-0.02
15,000	146	3.1 F	1.2 F	0.8 A	12.5 F/L	1.80	0.05
10,000	138	2.3 F	0.6 A	3.6 F	11.2 L	1.80	0.07
18,000	138	0.4 F/L	6.8 A	12.0 A	4.1 F	1.70	0.30

[1] Letter after flapping magnitude indicates approximate azimuth of largest down flapping.

A - Aft

A/L - Aft and Left

F - Forward

F/L - Forward and Left

L - Left

For the constant time point control inputs used, higher flapping peaks in the low-g portion of the maneuver usually resulted for the aft cg. The decreased pitch stability required the control inputs at the set time points to be larger than for forward cg to avoid overshooting the desired g-level. This results in larger magnitude pitch rates and stronger roll coupling that must be neutralized by more left lateral cyclic stick and consequent down left flapping.

The primary effect of gross weight changes was on the high-g portion of the maneuver. A heavier gross weight required a larger control input to attain the required pitch rate, and the blade stall effect was increased since the rotor was close to its thrust limit. In fact, the aircraft could not attain less than 0.3 g because of the severe aft flapping in the pushover. At light gross weight, the flapping due to blade stall was minor, and the low-g flapping was comparable to that seen at medium gross weight.

5.1.4 Effect of Hub Restraint

The effect of hub restraint on the teetering rotor system during this roller-coaster maneuver is presented in Table 10 for forward, mid, and aft center of gravity locations. For a given cg location, the primary effect of hub restraint is to significantly reduce the flapping in the low-g portion, with a relatively small change in high-g flapping. This results from the increased roll control power available with hub restraint over that which is available with the teetering rotor alone. Figure 20 presents the mid-cg low-g flapping peaks as a function of hub restraint. Note that a significant reduction in flapping is attained with a relatively small amount of hub restraint. The equivalent hinge offset shown in Figure 20 is the calculated articulated hinge offset required to attain the same flapwise natural rotor frequency as the two-bladed teetering rotor with hub restraint.

The minimum g level attained during the pushover also strongly affected the flapping peaks. Figure 21 shows the effect of g level on peak flapping for several levels of hub restraint. Note that for no hub restraint, the flapping tends to increase significantly just below zero g. With hub restraint, this increase is delayed to a more negative g level. This reflects the tendency of the basic rotor aerodynamic thrust control power to reverse with negative thrust on the rotor. With negative thrust, left swashplate input would give down left flapping but a right rolling moment about the aircraft cg. Hub restraint tends to cancel this reversed moment until the negative thrust becomes too large. Thus hub restraint merely delays the high flapping to lower g levels but does not eliminate it.

TABLE 10. EFFECT OF HUB RESTRAINT ON FLAPPING IN ROLLER-COASTER MANEUVER AT 140 KNOTS.

Utility Helicopter, Two-Bladed Teetering Rotor, GW = 15,000 lb

cg Location (in)	Hub Restraint $\left(\frac{\text{ft-lb}}{\text{deg}}\right)$	Flapping Peaks[1]				Max. Load Factor (g)	Min. Load Factor (g)
		Trim (deg)	Initial (deg)	Second (deg)	Low g (deg)		
138	0	1.2 F	3.0 A	5.9 A	10.8 L	1.80	0.12
138	100	1.2 F	5.6 A	5.3 A	10.6 L/A	1.80	0.12
138	200	1.2 F	2.8 A	5.6 A	10.0 L/A	1.82	0.12
138	400	0.9 F	3.2 A	6.0 A	7.1 L/A	1.82	0.15
138	1000	0.9 F	2.6 A	5.0 A	3.9 L/A	1.80	0.28
130	0	1.7 L/A	8.4 A	9.7 A	8.9 L	1.85	-0.02
130	40	1.7 L/A	8.8 A	8.9 A	8.4 L	1.75	0.07
130	100	1.6 L/A	8.1 A	9.0 L/A	7.1 L/A	1.75	0.10
130	200	1.5 L/A	8.3 A	9.0 L/A	7.0 L/A	1.75	0.10
130	400	1.4 L/A	8.4 A	9.4 L/A	5.2 L	1.75	0.15
130	1000	1.2 L/A	6.0 A	6.2 L/A	4.4 L/A	1.75	0.08
146	0	3.1 F	1.2 F	0.8 A	12.5 L/F	1.75	0.05
146	100	3.2 F	1.0 L/F	1.0 A	8.0 F	1.77	0.10
146	200	3.0 F	0.8 F	1.0 A	6.2 L/F	1.80	0.15
146	400	2.9 F	0.8 F	1.0 A	6.0 L/F	1.80	0.08

[1]Letter after flapping magnitude indicated approximate azimuth of largest down flapping

A - Aft
F - Forward
L - Left
L/A - Left and Aft
L/F - Left and Forward

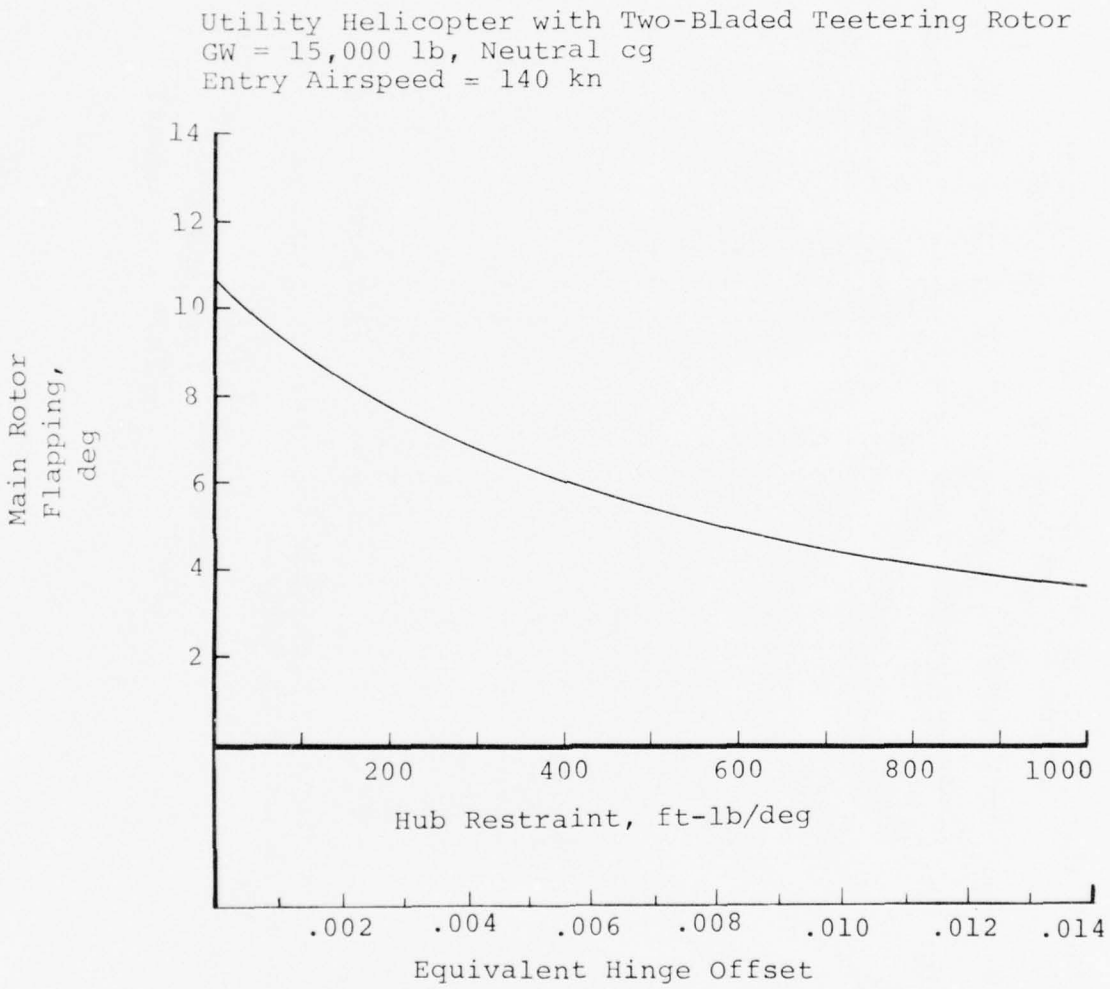

Figure 20. Effect of hub restraint on low-g flapping in roller-coaster maneuver.

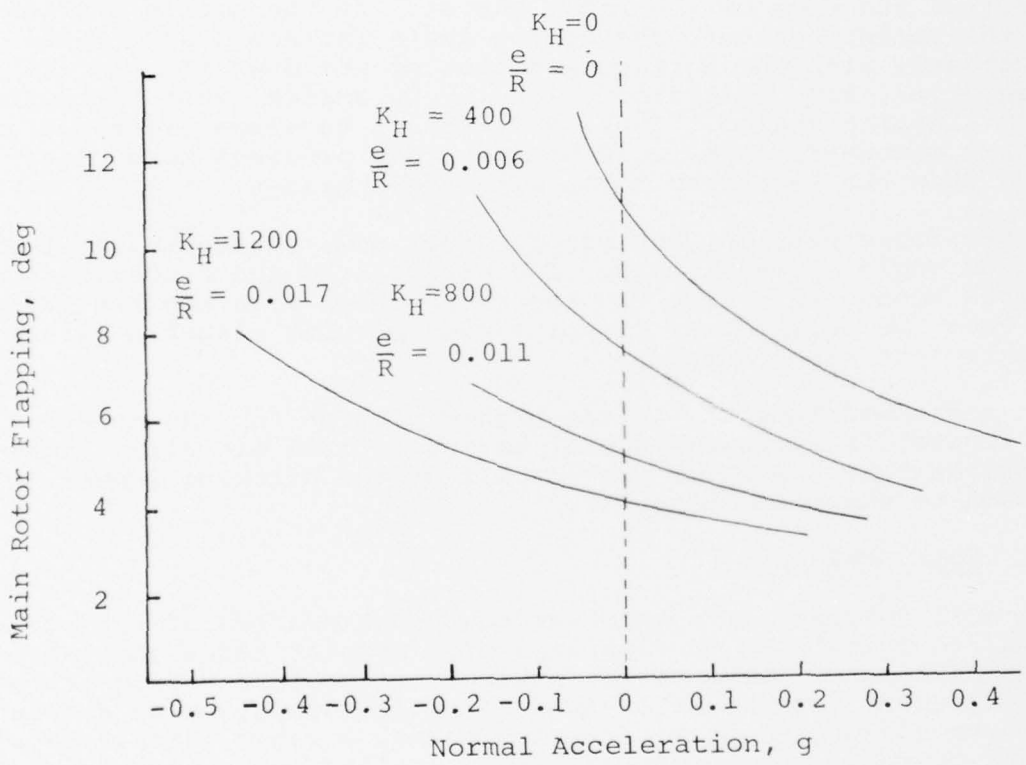

Figure 21. Effect of minimum-g level in roller-coaster maneuver.

5.1.5 Effect of Helicopter and Rotor Type

Helicopter type did not affect these trends (Table 11), but for the articulated and hingeless rotor systems, the introduction of a coning angle became significant. The two-bladed teetering rotor has a preset coning angle due to the rigid hub connecting the two blades. However, the effective flapping hinge of the articulated and hingeless rotors will allow the blades to move individually and flap about a mean coning angle that is primarily a function of the rotor thrust. In the high-g portion of the roller coaster, the coning angle increased as g-level increased, with the consequence that no net down flapping is seen (i.e., the oscillatory flapping is smaller than the positive mean flapping angle). Thus, in terms of fuselage clearance in high-g maneuvers, the rigid hinged blade provides more clearance than the teetering rotor with rigid blades.

In the low-g portion, the rotor thrust and, consequently, the coning angle approach zero. The articulated and hingeless rotors become more like the teetering rotor with hub restraint in that the oscillatory flapping peak becomes almost a direct function of hub restraint.

The increased flapping in the high-g portion for the observation helicopter is a consequence of having a fixed elevator. This requires that the rotor provide all of the pitching moment needed to start the maneuver.

5.2 ROLL REVERSALS

The roll reversal is a maneuver that combines two of the principal contributions to flapping: high angular rates and large control inputs. Each of the subject helicopters was run through a structural demonstration-type maneuver consisting of a slow roll to ≈45-degree bank; at which point, a rapid lateral cyclic input in the opposite direction was applied to generate a peak roll rate of ≈70 degrees/second in the opposite direction. The stick was then rapidly returned to approximately neutral to stop this maneuver. A time history of a typical roll reversal is given in Figure 22. Notice that even though the second control input is of about the same magnitude as the first, the second flapping peak is higher, as would be expected for the rotor lag plus swashplate input.

Table 12 lists the flapping angles during this maneuver for all six helicopters. Each helicopter follows the general trend that the second flapping peak is larger than the first except when the initial roll is towards the left. Rotor coupling provides a higher thrust level for reversals that begin towards the right, requiring less lateral control input to attain the desired roll rates.

TABLE 11. FLAPPING IN ROLLER-COASTER MANEUVER FOR DIFFERENT HELICOPTER AND ROTOR TYPES

Type[1] (-)	cg Location (in)	Flapping Peaks[2]				Max. Load Factor (g)	Min. Load Factor (g)
		Trim (deg)	Initial (deg)	Second (deg)	Low g (deg)		
ART	138	2.8±1.6 F	4.1±0.6 A	3.0±2.2 A	1.0±3.0 F	1.88	0.06
HNG	138	2.6±1.1 F	3.7±0.4 A	3.7±2.5 F	0.8±1.0 F	1.77	0.09
OH	110	2.2F	6.0A	-	8.8F	1.85	0.10
OH	104	1.3A	10.0A	-	6.6F	1.80	0.08
OH	116	5.6F	2.0A	-	11.7R	1.90	0.14
AH	195	0.8 L/A	5.2A	7.2A	7.2R	1.90	0.11
AH	190	3.2A	7.2A	8.8A	6.5R	1.75	0.07
AH	200	1.0F	3.0A	5.2A	9.0R	1.85	0.11

[1]Type of Rotor or Helicopter:

ART - Articulated four-bladed rotor on UH fuselage, 15,000 lb Gross Weight

HNG - Hingeless four-bladed rotor on UH fuselage, 15,000 lb Gross Weight

OH - Teetering two-bladed rotor, 3000 lb Gross Weight

AH - Teetering two-bladed rotor, 14,000 lb Gross Weight

[2]Letter after flapping magnitude indicates approximate azimuth of largest down flapping

A - Aft

F - Forward

R - Right

L - Left

L/A - Left and Aft

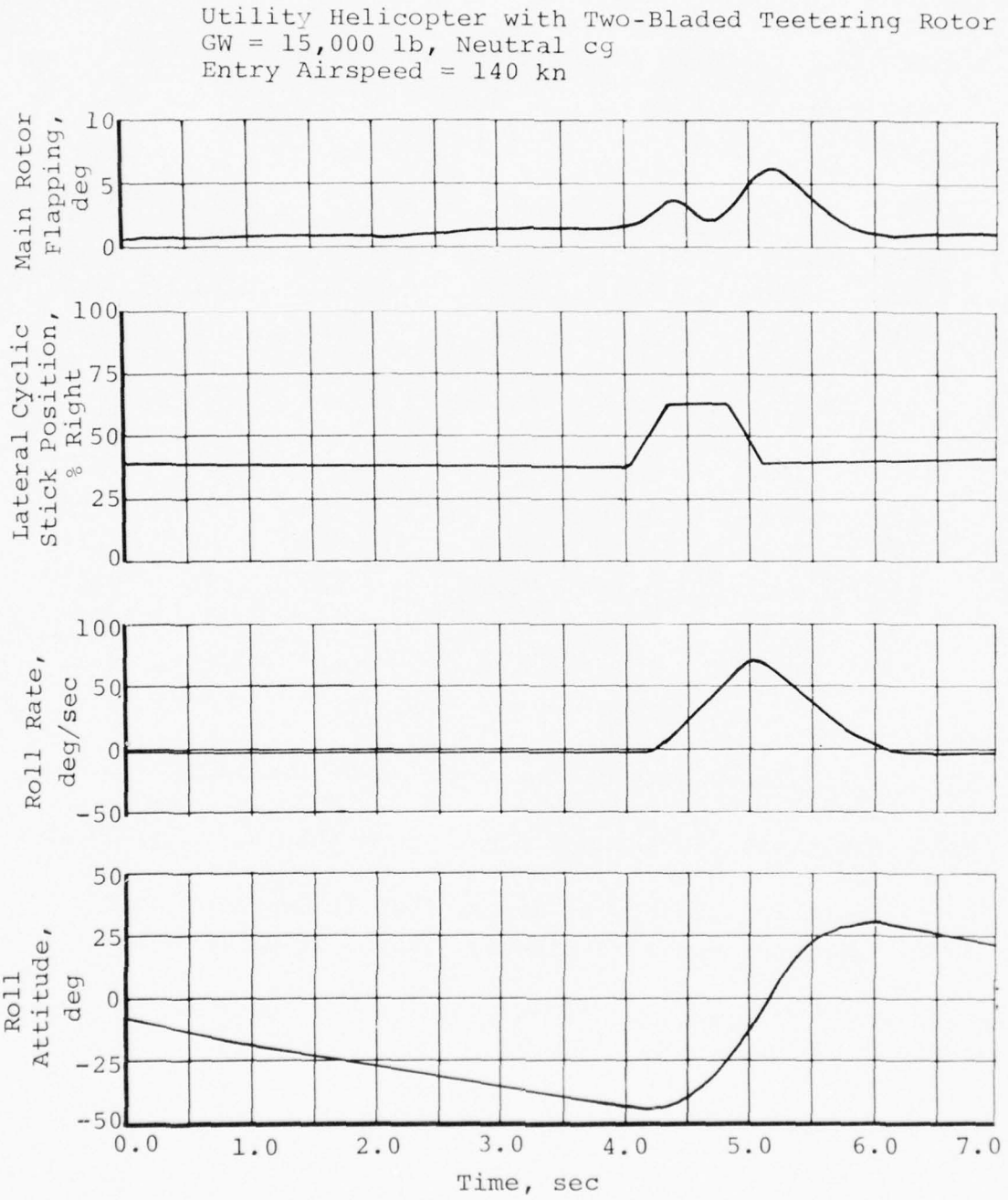

Figure 22. Typical roll reversal maneuver.

TABLE 12. EFFECT OF HELICOPTER TYPE ON ROLL REVERSAL MANEUVER

Helicopter (-)	Rotor[1] (-)	Gross Weight (lb)	cg Location (in)	Hub Restraint ft - lb / deg	Direction of Maneuver[2] (-)	Flapping Peaks[3] Trim (deg)	First (deg)	Second (deg)
UH	2T	15,000	138	0	L to R	2.2 F	6.6 L/A	6.6 R/A
UH	2T	15,000	138	0	R to L	1.5 R/F	4.2 R	7.8 L
UH	2T	15,000	138	400	R to L	1.2 F/R	3.6 R	5.8 L/F
UH	2T	15,000	138	400	L to R	1.6 F/R	5.3 L/F	6.0 R/A
UH	4A	15,000	138	1032	L to R	2.0 ±2.7R/F	3.0 ±4.7L	4.0 ±3.0R
UH	4A	15,000	138	1032	R to L	2.0 ±2.4F	2.4 ±3.6R	3.9 ±3.7L/F
UH	4H	15,000	138	2428	R to L	2.1 ±1.5R/F	2.3 ±1.9R/F	3.6 ±3.3L/F
UH	4H	15,000	138	2428	L to R	1.9 ±1.5R/F	2.4 ±3.0L/F	3.6 ±2.4R/A
AH	2T	14,000	195	0	L to R	1.2 L	4.2 L	9.9 R
AH	2T	14,000	195	0	R to L	0.8 L	1.2 R	10.5 L
OH	2T	3000	110	0	L to R	5.0 R/F	6.6 F	7.8 R/A
OH	2T	3000	110	0	R to L	5.0 F	5.8 L	6.8 R

NOTE: All 'UH' helicopters were at 140 knots, 'AH' helicopters at 160 knots, and 'OH' helicopters at 120 knots.

[1] Number and letter indicate type rotor as follows:
2 - Two-bladed; 4 - Four-bladed; T - Teetering; A - Articulated; H - Hingeless

[2] Letter indicates: L - Left; R - Right

[3] Letter after flapping magnitude indicates approximate azimuth of largest down flapping: A-Aft; F-Forward; R-Right; L-Left; L/A-Left and Aft; R/F-Right and Forward; R/A-Right and Aft; L/F-Left and Forward.

A different maneuver, in which the step input was not removed, was performed to evaluate the effect of longitudinal center of gravity location on the roll reversal. The helicopter was rolled to a bank angle in one direction and a lateral cyclic step input was applied in the opposite direction. The same magnitude input was used for all cases listed in Table 13. Slightly higher flapping peaks are noted at the aft cg, and the flapping to the left is always more than that for steps to the right.

5.3 AUTOROTATION ENTRIES

Autorotation entries were run for each helicopter to obtain a comparison in high-speed flight at large sideslip angles. A typical autorotation entry is presented in Figure 23 and is characterized by several flapping peaks. The first peak occurs at the throttle chop when the main rotor torque is suddenly reduced. The fin and tail rotor are still providing a force to the right to oppose rotor torque, consequently the tail of the aircraft swings to the right. The natural dihedral effect of the rotor will normally cause the fuselage to roll left with the resultant nose left sideslip. Right cyclic stick inputs by the SCAS attempt to maintain the trim roll angle, and these cyclic inputs result in a small flapping peak. If SCAS is not on, the helicopter will enter a left turn and will not flap significantly. It should be noted that the initial reaction will be a strong function of the dihedral effect of the fuselage, as discussed in the parametric study, and of the amount of torque that is needed to drive the main rotor before the throttle chop.

The rpm decay rate determines how much delay is possible before the recovery is started. A two-second delay was possible on all but the AH helicopter, which was flying faster and at higher torque settings than the other aircraft. At the end of the delay, the collective pitch was reduced, and aft cyclic stick applied to initiate a flare to regain main rotor rpm. The rate and magnitude of these control inputs controlled the amount of flapping seen in this portion of the maneuver. This simulation used inputs that would successfully arrest the rpm decay and initiate 10- to 15-degree nose-up flare. It was during this flare maneuver that the largest flapping peaks occurred. An initial peak was in response to the cyclic input, but the SCAS and autopilot had a tendency to overcontrol and usually one or two cycles of a decaying pitch and roll oscillation occurred. A second flapping peak sometimes occurred during the settling of these oscillations that was a direct function of the SCAS and autopilot cyclic commands. While these pitch and roll oscillations may not be totally representative of operational systems, they again illustrate the relation between flapping and control inputs.

TABLE 13. EFFECT OF CENTER OF GRAVITY LOCATION ON RESPONSE TO LATERAL CONTROL INPUTS

Utility Helicopter, Two-Bladed Teetering Rotor, GW = 15,000 lb, Airspeed = 140 Kn

cg Location (in.)	Lateral Cyclic Input[1] (deg)	Trim Flapping[2] (deg)	Peak Flapping[2] (deg)
138	7.2 L	0.7 F	7.1 L/F
138	7.2 L	1.0 F	7.4 L/F
138	7.2 L	0.8 F	7.0 L/F
138	7.2 R	0.7 F	5.8 R/A
138	7.2 R	0.7 F	5.7 R/A
130	7.2 R	1.7 A	5.8 R/A
130	7.2 R	1.7 A	5.8 R/A
130	7.2 R	1.7 A	6.0 R/A
130	7.2 L	1.7 A	7.6 L/F
130	7.2 L	1.7 A	7.6 L/F
148	7.2 L	3.0 F	8.0 F/L
148	7.2 L	3.0 F	8.0 F/L
148	7.2 R	3.0 F	6.2 R/A
148	7.2 R	3.0 F	6.1 R

[1] Letter after number indicates: L - Left, R - Right

[2] Letter after flapping magnitude indicates approximate azimuth of largest down flapping:

A - Aft
F - Forward
R - Right
L - Left
L/F - Left and Forward
L/A - Left and Aft
R/F - Right and Forward

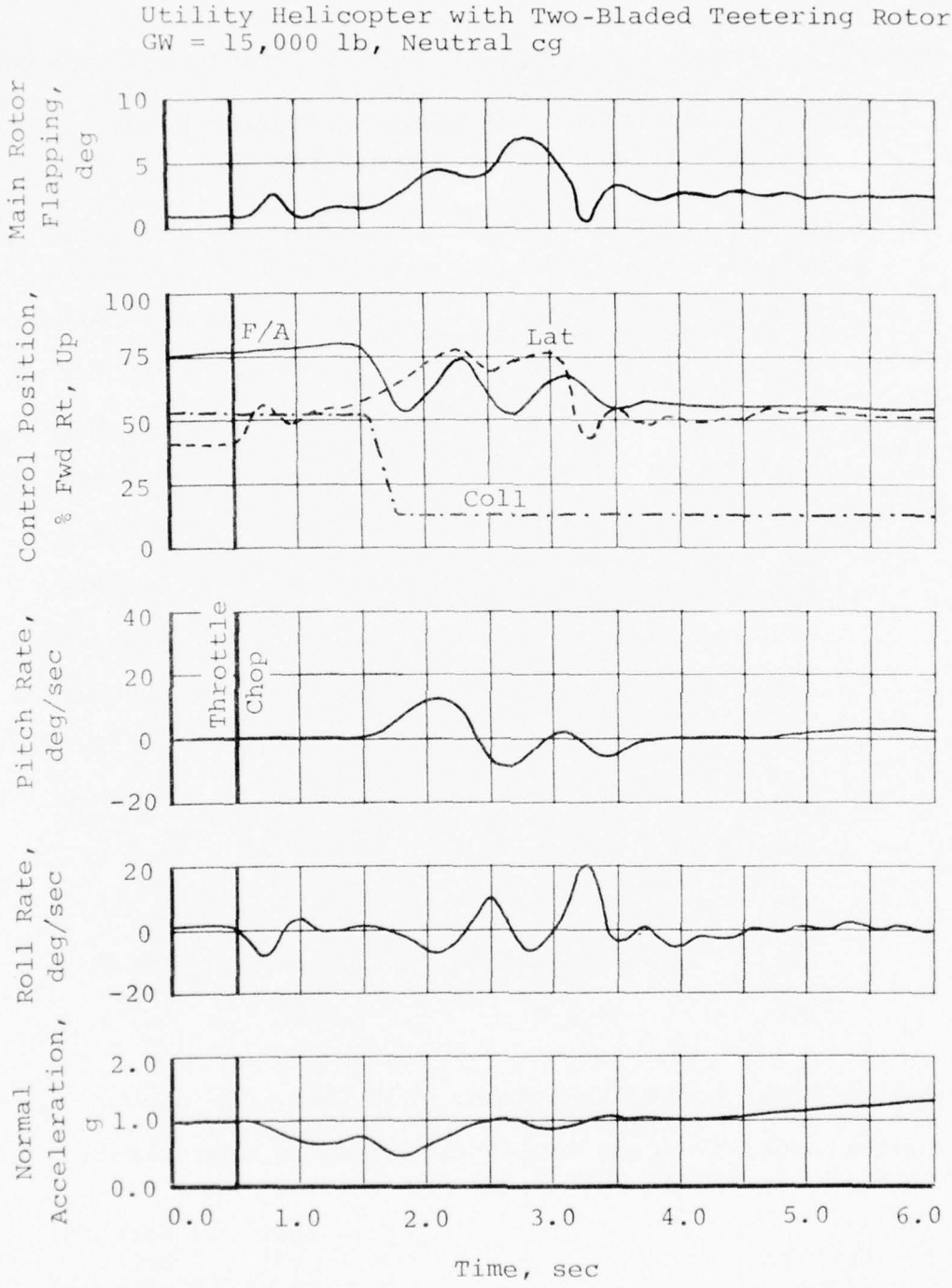

Figure 23. Typical autorotation entry maneuver.

A tabulation of flapping peaks during an autorotation entry of each helicopter is given in Table 14. In the UH series, the oscillatory flapping peaks decrease with increasing effective hub restraint. The effective hub restraint is increased as the rotor type is changed from teetering to articulated to hingeless. The AH autorotation entry was made at 160 knots; however, the 2-second delay before the collective drop could not be attained. With a 1-second delay, the maneuver was successfully run and, when repeated at 140 knots, gave reduced flapping in the flare portion.

All of the simulated helicopters exceeded 7 degrees of sideslip during these high speed autorotational entry maneuvers. In all cases, no significant flapping increase was noted until the recovery control inputs were made.

5.4 HIGH HOVER AUTOROTATIONAL ENTRY

This maneuver consists of a throttle chop from an out-of-ground-effect hover, followed, after a two second delay, by a collective stick drop and a rapid forward cyclic input. The objective was to reach a nose down pitch rate of 15- to 20-degrees per second in order to attain a pitch attitude of 25- to 30-degrees nose down as soon as possible. This maneuver was to gain airspeed to allow a normal autorotational approach to a landing at about 60 knots forward airspeed. The landing was not to be simulated, and the maneuver was to be terminated as soon as it was felt that steady autorotative flight could be attained. However, the simulation of the entire maneuver was not satisfactorily completed in the time available, thus no time history is presented.

The response of the ship to this maneuver was a highly coupled reaction to the rapid control inputs required after the 2-second delay. The simulator autopilot tended to overcorrect for aircraft attitude errors, and a rolling, pitching, and yawing oscillation was usually encountered that would go through at least two cycles before settling. During these oscillations, large control inputs were being made and flapping peaked to over 9 degrees.

This maneuver could have been controlled better if the simulator and autopilot gains were adjusted. However, it was felt to be representative of the type an inexperienced, over-controlling pilot could encounter. Large control inputs at inappropriate times led to high flapping peaks.

5.5 TAIL ROTOR LOSS

The loss of a tail rotor was simulated by simultaneously setting the tail rotor thrust to zero and dropping 100 pounds from the tail rotor location. This would approximate the loss of the tail rotor blades and the 90-degree gearbox.

TABLE 14 - FLAPPING IN AUTOROTATIONAL ENTRIES

Heli-copter[1] (-)	Rotor[2] (-)	Airspeed at Entry (Kn)	rpm Decay Rate (rpm/sec)	Flapping[3] Trim (deg)	At Coll. Drop (deg)	Initial Peak (deg)	Second Peak (deg)
UH	2T	140	-36	1.7A	3.3A	6.8A	8.3A
UH	4A	140	-42	3.0±0.9F	2.4±1.7A	2.5±4.6A	2.8±4.0A
UH	4H	140	-42	2.7±0.6F/R	2.0±1.5A	2.4±3.7A	3.3±3.8A/L
AH	2T	160	-36	2.6 A/L	4.6 A/R	8.8A	9.2A
AH	2T	140	-28	2.8A	4.1A	7.7A	5.6A
OH	2T	120	-41	0.4R	2.9A	10.1A	9.6A

[1]All helicopters at medium gross weight and forward cg.

UH - GW = 15,000 lb, cg = 130 in. AH - GW = 14,000 lb, cg = 190 in. OH - GW = 3000 lb, cg = 104 in.

[2]Number and letter indicate type rotor as follows:

2 - Two-bladed; 4 - Four-bladed; T - Teetering; A - Articulated; H - Hingeless

[3]Letter after flapping magnitude indicates approximate azimuth of largest down flapping: A-Aft; F-Forward; A/R-Aft and Right; A/L-Aft and Left; F/R-Forward and Right, R-Right.

The initial runs were made at 100 knots cruising flight for the UH with a two-bladed teetering rotor. The fin size of the basic helicopter was found to be inadequate to stop the initial yaw rate developed due to the loss of the antitorque contribution of the tail rotor. The helicopter would yaw to an attitude from which recovery was impossible. The fin size was increased to allow this maneuver to be completed. A typical tail rotor loss maneuver is shown in Figure 24.

Upon tail rotor loss, the ship immediately started to yaw nose right, pitch nose down, and roll slightly to the left. SCAS inputs tend to reduce roll and pitch changes that are mild. The main rotor flapping increased only slightly even when the sideslip angle reached 13 degrees or more. After a 2-second delay, the collective was lowered and a cyclic flare initiated in order to reduce the airspeed and relieve the antitorque requirement on the fin. As was noted in previous autorotation entry conditions, at this point, large rapid control inputs can result in large flapping peaks. The results of these maneuvers at two airspeeds are listed in Table 15.

Since little difference was noted between the flapping reaction to tail rotor loss or autorotation entries, the autorotation entry was used for comparison between helicopters for the high sideslip flight condition.

5.6 POWER-ON FLARE

The power-on flare maneuver was a constant altitude deceleration from level flight to a hover. From trimmed flight at 100 knots, aft cyclic stick was used to initiate a 20-degree nose-up flare while simultaneously adjusting collective to control the main rotor rpm. Once airspeed was down to about 10 knots, the helicopter was nosed over to a hover. The altitude change during this maneuver was held to less than 10 feet.

An initial peak of 7 degrees down aft flapping occurred when the initial cyclic input was made, and except for smaller peaks caused by the final adjustments of pitch attitude, the flapping decreased steadily. At hover entry, a smaller flapping peak occurred when control inputs were used to nose over to a hover.

Since the flapping peak at the low-speed end of the maneuver was small, subsequent runs were made for only the initial flare from level flight.

A 400-ft-lb/deg hub spring was added, and the maneuver was repeated using the same longitudinal cyclic inputs. The same pitch attitude resulted, and the initial flapping peak was indistinguishable from that obtained with no hub spring.

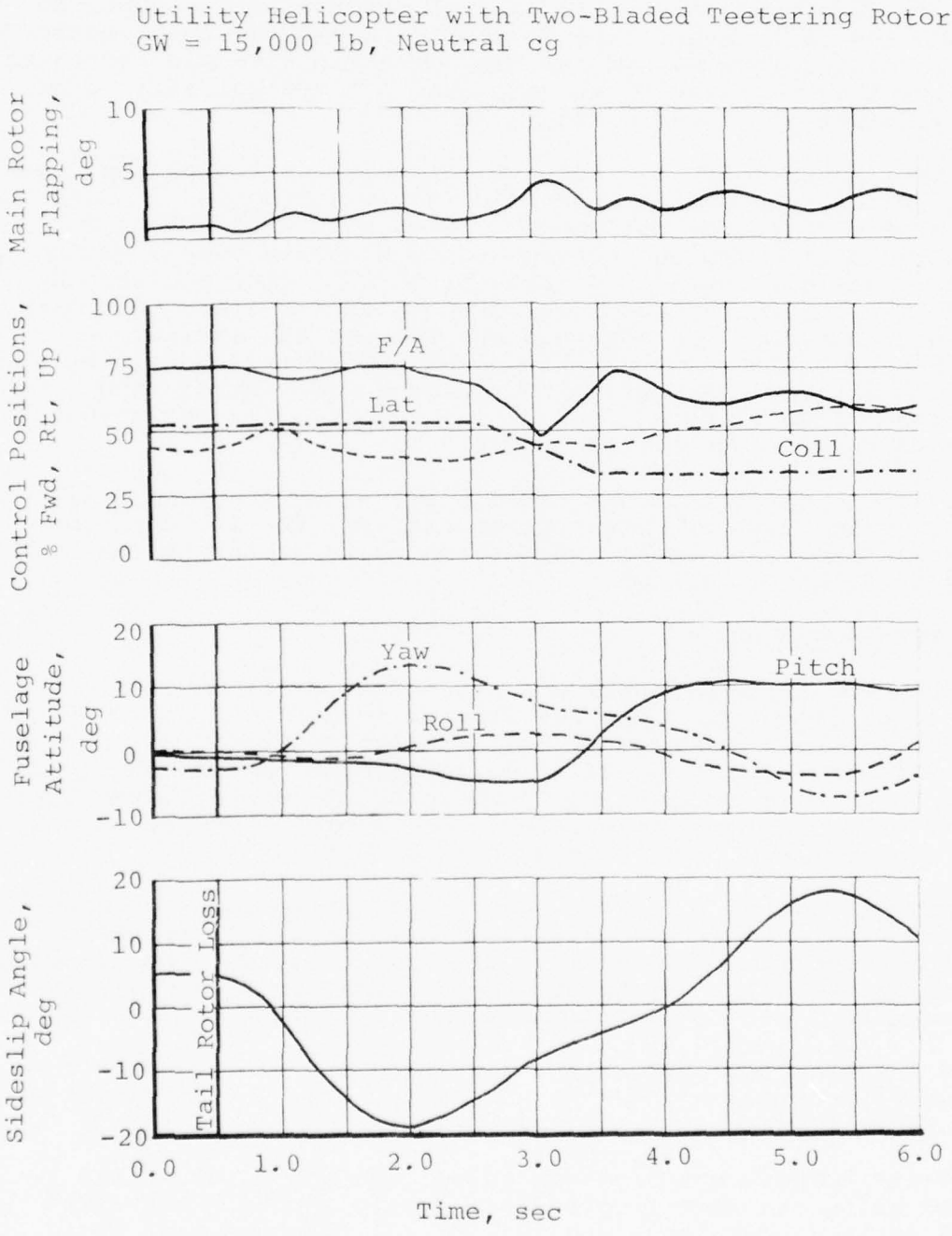

Figure 24. Typical tail rotor loss maneuver.

TABLE 15 - FLAPPING IN TAIL ROTOR LOSS

Utility Helicopter, Teetering Rotor 15,000 lb,
Neutral cg

Airspeed (Kn)	Trim Flap[1] (deg)	Peak Flapping[1] Before Coll Drop (deg)	Peak Flapping[1] After Coll Drop (deg)	Peak Sideslip (deg)
100	0.8A	1.8A	-	>20
140	0.8F	2.2R	4.8A	>12

[1]Letter after flapping magnitude indicates approximate azimuth of largest down flapping

A - Aft
F - Forward
R - Right

The zero hub spring helicopter repeated the maneuver at 18,000 pounds gross weight using the same longitudinal cyclic stick inputs as for 15,000 pounds. The major effect of the increased gross weight was a more rapid increase in collective stick to hold the rpm up. The flapping peak on entry decreased only 0.6 degrees from that measured at the lighter weight.

The last effect investigated was the movement of the center of gravity forward. The flapping peak at forward center of gravity was increased over that seen at neutral center of gravity. This increase was of the same magnitude as the trimmed flight flapping increase due to the center of gravity shift. For this case, the superposition of center of gravity effect on trim could be used to predict this flapping.

5.7 POWER-OFF FLARE

The power-off flare was entered from a steady autorotation at 60 knots. An aft cyclic control input was made to bring the nose of the ship to about 20 degrees nose-up to flare for an autorotational landing. The flare was simulated from initiation to about 15 knots airspeed but no landing was attempted. The flapping characteristics were similar to those noted in the power-on flare.

The peak flapping during this maneuver occurred immediately after the initial control input and was a function of both the rate and amplitude of the longitudinal cyclic input. Figure 25 summarizes this relationship for the power-off flare maneuver and was determined in the following manner. A triangular longitudinal cyclic input was found that gave a steady 20-degree nose-up pitch attitude. Holding the product of the peak amplitude and the length of time the control was applied constant, it is seen that many combinations of amplitude and time produce the same final pitch attitude. A large magnitude control input applied over a short time results in high pitch rates and high flapping to reach to the 20-degree attitude. A lower magnitude input applied over a larger time reaches the same pitch attitude but with a lower pitch rate and lower flapping.

This result agrees with comments by experimental test pilots at BHT and supports the idea that slow, deliberate control inputs are necessary to recover from unusual flight attitudes. Large, rapid control inputs should not be used if high flapping is to be avoided.

5.8 HOVERING POP-UP

This maneuver consisted of a rapid collective input to attain approximately 1.5g normal acceleration from hover at extreme longitudinal center of gravity loading (Figure 26). The reaction of the main rotor flapping was, for the extreme forward

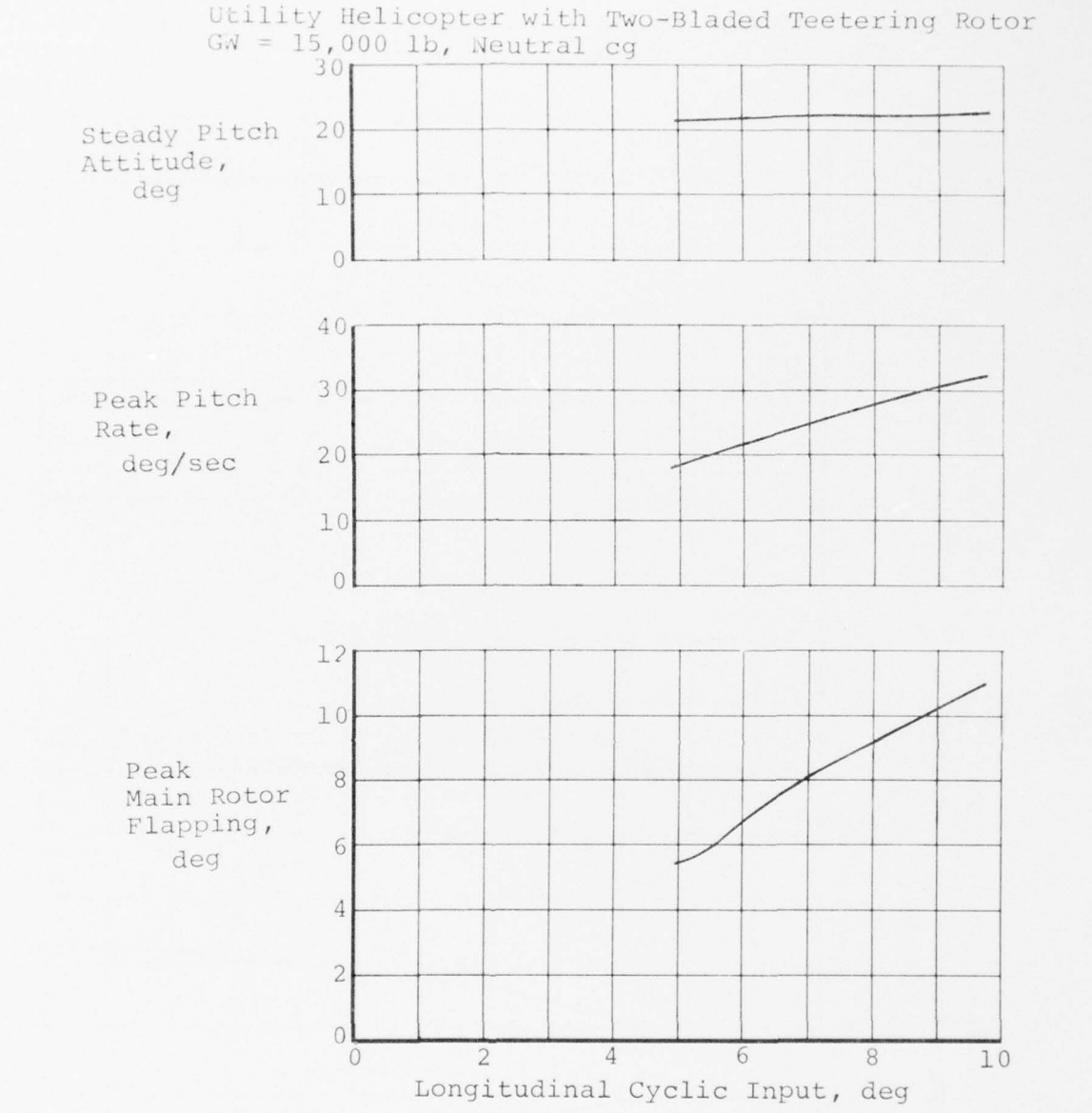

Figure 25. Effect of control input magnitude and rate on main rotor flapping.

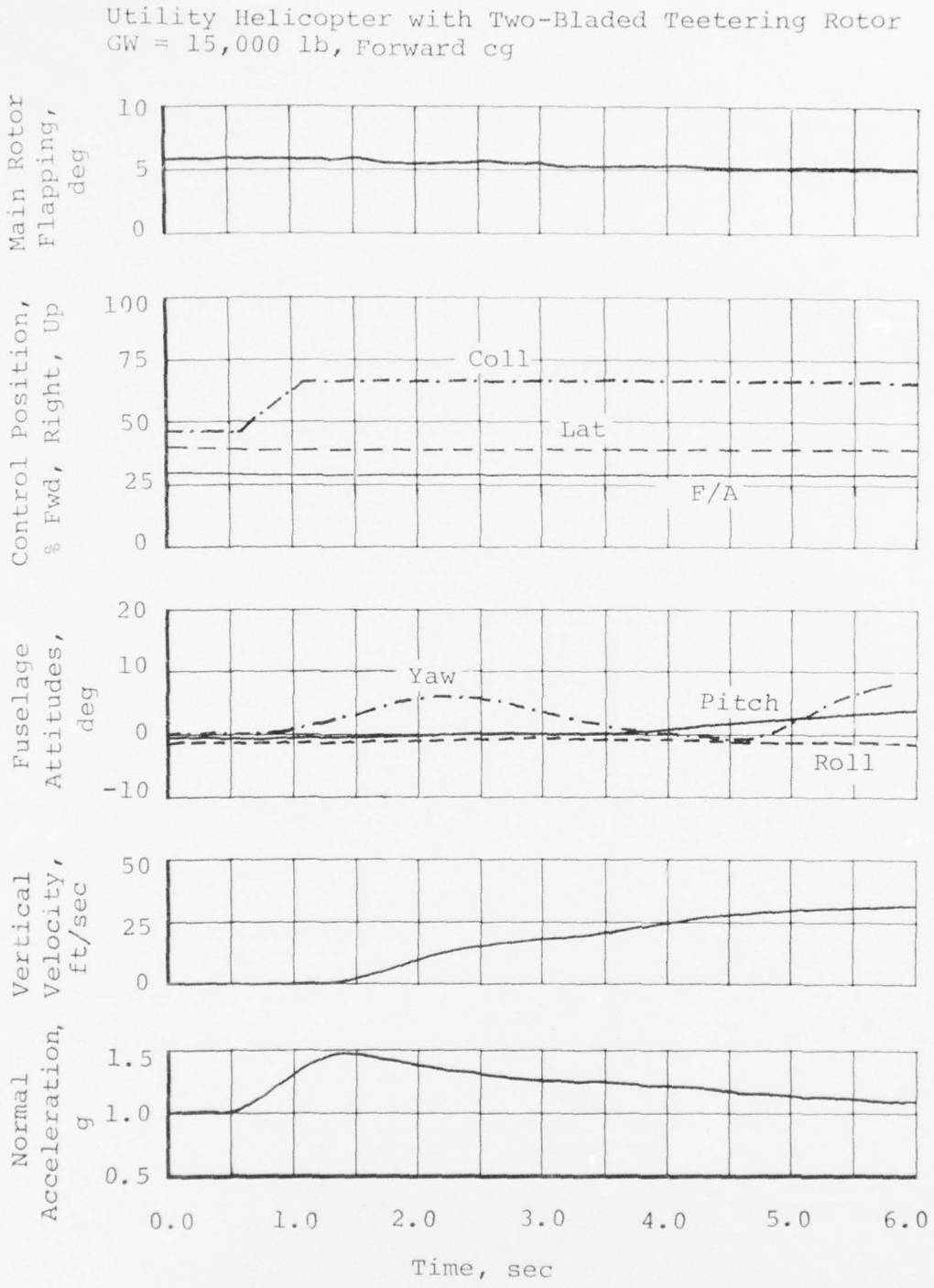

Figure 26. Typical pop-up from hover.

center of gravity, a steady decrease in magnitude as the rate of climb increased. At aft center of gravity, the flapping gradually increased. For both cases, the download on the elevator will build up as the rate of climb increases, causing a nose-up pitch rate to develop. This will lead to nose-down flapping that will produce the tendencies described above. No transient flapping peaks were seen in this maneuver.

5.9 HARD LANDINGS AND JUMP TAKEOFFS

Using a simple landing gear model in hybrid C81, hard landings were simulated with a vertical descent to ground contact. The sink rate at touchdown was set by reducing the collective pitch setting below that required for hover and descending from about a 10-foot skid height. After touchdown, the collective was lowered to flat pitch and held down until transient oscillation died out. Since jump takeoffs were also to be run, the end of the maneuver was a collective pull-up and a vertical takeoff.

At the aft center of gravity, the aft left gear hit first and generated an initial right roll rate and nose-down pitch. When SCAS was on, these large rates generated large control inputs (to the limit of SCAS authority) to attempt to neutralize the rates. The fuselage pitch rate was particularly large when compared to rates seen in normal flight, and when the normal rotor lag plus the SCAS control input is made, large flapping magnitudes result. When the pitch channel of SCAS is inoperative, the flapping in the hard landing is reduced. Figure 27 is a hard landing with pitch SCAS on, and Figure 28 is the same maneuver with pitch SCAS off. A reduction of about 2 degrees (approximatley one-half the SCAS authority) is seen in the second flapping peak after touchdown with the SCAS off.

The trend of increased flapping with pitch SCAS on is present at all sink rates used and for both forward and aft cg extremes. Table 16 lists the data obtained in the hard landing portion of these maneuvers for variations in sink rate and center of gravity location with SCAS on and off.

The jump takeoff at aft center of gravity showed a similar trend of flapping to that seen at forward center of gravity. The cyclic stick was positioned near the middle of its range before the collective was moved. When the aircraft started to lift off, a nose up pitch rate developed. The pitch SCAS applied forward cyclic to counteract this rate, and this combination produced down forward flapping. With the SCAS off, the same maneuver produced about 3 degrees less flapping. These trends are illustrated in Figures 27 and 28 for the aft center of gravity loadings. When a jump takeoff was made for the forward center of gravity, the above trends were repeated but with a nose down pitch rate and down aft flapping peaks.

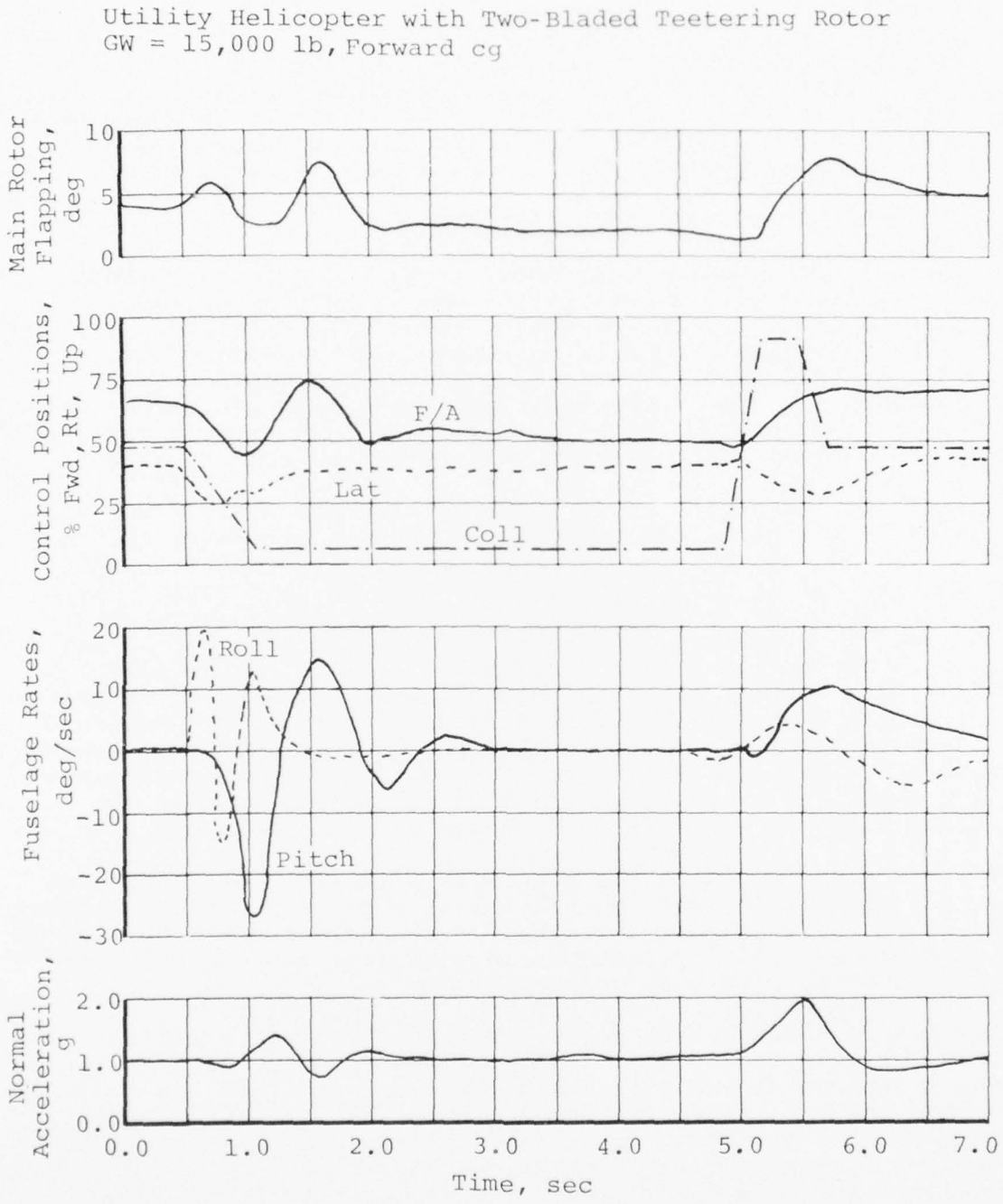

Figure 27. Typical hard landing and jump takeoff - SCAS on.

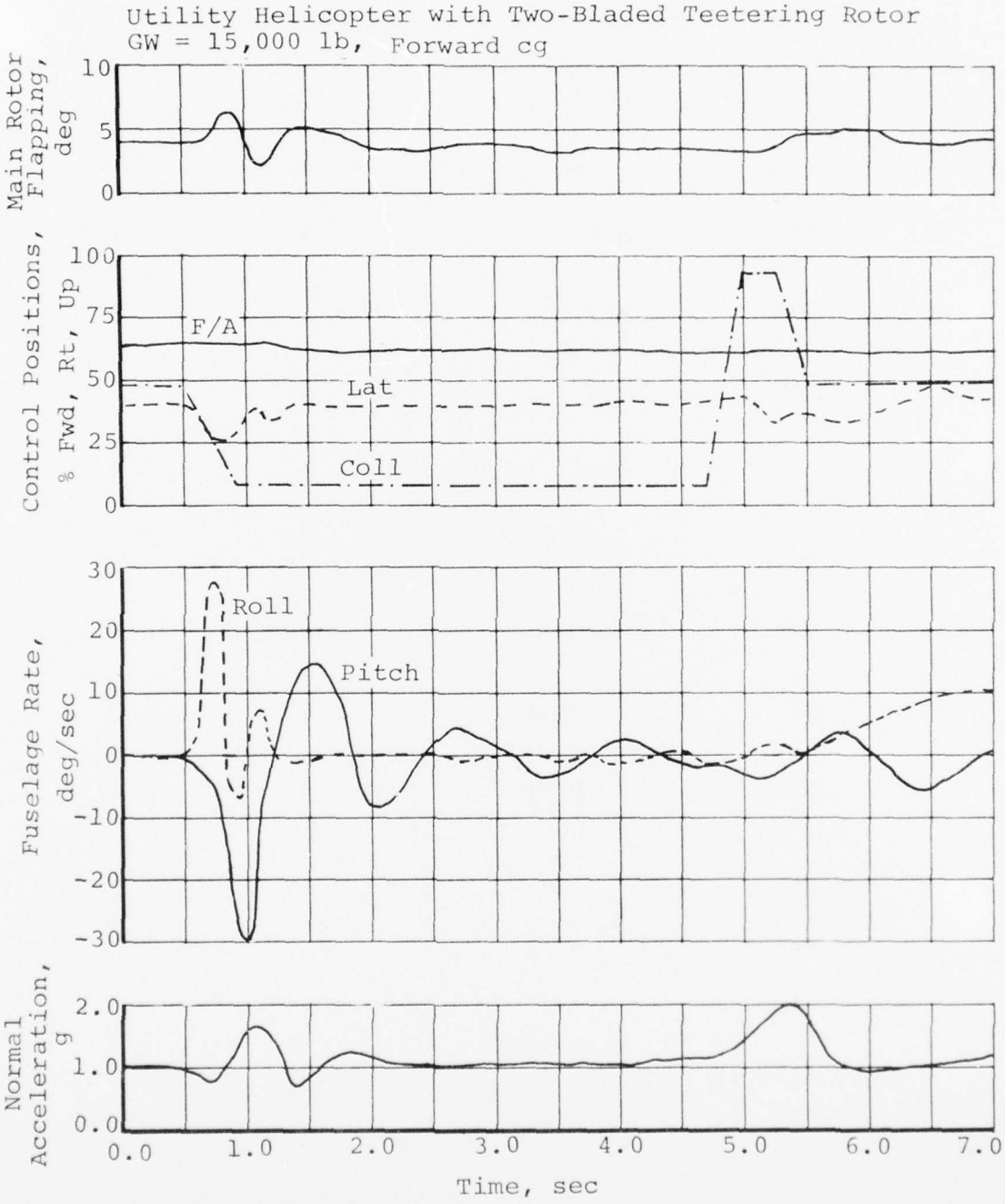

Figure 28. Typical hard landing and jump takeoff - SCAS off.

TABLE 16. FLAPPING IN HARD LANDINGS FROM HOVER

Utility Helicopter, Two-Bladed Teetering Rotor, GW = 15,000 lb

Rate of Sink (ft/sec)	SCAS	Center of Gravity Location	Flapping in Hover (deg)	Peak Flapping (deg)
- 5	ON	AFT	4	9.5
- 5	OFF	AFT	4	6.6
-10	ON	AFT	4	12.0
-10	OFF	AFT	4	8.3
- 5	ON	FORWARD	6	11.0
- 5	OFF	FORWARD	6	8.0
-10	ON	FORWARD	6	≈13
-10	OFF	FORWARD	6	6.6

6. CRITICAL FLIGHT CONDITION RESULTS

The results of the critical flight condition simulation and the parametric study have indicated flight conditions, control inputs, and helicopter characteristics that tend to affect main rotor flapping.

6.1 CRITICAL FLIGHT CONDITIONS

Flight conditions associated with high flapping were low or negative-g conditions and areas where significant retreating blade stall occurs. Low-g conditions were a problem for helicopters without hub restraint since the rotor thrust would approach zero and, since lateral control is obtained by directing this thrust vector, the lateral control power would also approach zero. Even with hub restraint, a negative-g level will be reached at which the cyclic controls will become ineffective or reversed. Hub restraint merely moves this g level to more negative values.

Retreating blade stall occurs when the angle of attack on the retreating blade exceeds its stall limit, with a resultant decrease in lift and increase in drag. Conditions that cause significant amounts of blade stall are heavy gross weight, high load factors, high density altitude, high advance ratio (low RPM and/or high speed) and control inputs that tend to increase the angle of attack on the retreating blade.

6.2 CRITICAL CONTROL INPUTS

Control inputs were a source of high flapping when made rapidly and with large amplitude. If the cyclic control is applied faster than the helicopter will respond, high flapping will result in proportion to this input. If control movements are made slowly so that the helicopter responds in its natural rigid body modes, little flapping is seen when even large fuselage responses are demanded.

Another identified source of control input was that of automatic stabilization equipment (SCAS) on hard landings in nose-high or nose-low conditions. The large fuselage rates upon ground contact tend to be much larger than rates seen in flight. The SCAS network, which is designed for airborne conditions, tends to give its full authority in the direction opposing the fuselage rate. This SCAS input causes higher flapping in hard landings than when the SCAS is off.

6.3 CRITICAL HELICOPTER CHARACTERISTICS

Many helicopter and rotor characteristics have been identified as affecting flapping in flight. However, three categories of characteristics are of particular importance:

6.3.1 Rotor Type

The three rotors investigated have similar characteristics in that the same control inputs and operating conditions that produce high flapping for one rotor will produce high flapping for the other types. The principal difference in flapping between the rotor types was produced by differences in effective hub restraint. The additional hub moment due to flapping restraint tends to rotate the fuselage in a direction tending to reduce flapping for all maneuvers. In addition, the control power provided at low- or negative-g levels reduced flapping significantly in this flight regime. It was also noted that the coning angle of the articulated and hingeless rotors approached zero in low-g maneuvers, tending to reduce rotor to fuselage clearance even with the high hub restraint.

6.3.2 Fuselage Stability

Fuselage stability characteristics affect flapping primarily in forward flight. Increased pitch stability requires larger control inputs and, consequently, higher flapping to achieve a desired pitch rate. Elevator gearing alters the pitch stability and, if geared to increase pitch control power, will reduce flapping in longitudinal maneuvers.

In low speed flight, the location of the elevator with respect to the main rotor wake can make a significant contribution to main rotor flapping. If the elevator is located such that the main rotor wake can impinge on the surface at low speeds, large pitching moments can be developed causing fuselage attitude changes and consequent changes in flapping.

Dihedral stability (rolling moment due to sideslip) will indirectly affect flapping in maneuvers. A nonneutral dihedral effect will cause roll when the aircraft is sideslipped, as in pedal kicks, autorotation entries or tail rotor loss. The lateral cyclic control, and thus flapping, required to counteract this roll will be proportional to the dihedral effect.

6.3.3 Loading Conditions

Helicopter loading conditions will affect flapping through both center of gravity and gross weight effects. Center of gravity extremes produce high flapping in low-speed flight due

to the fuselage attitudes required. In high-speed flight, the effect of the center of gravity on pitch stability, as discussed above, predominates. Heavy gross weights increase the possibility of encountering retreating blade stall in high speed flight maneuvers.

7. FLAPPING DESIGN CRITERIA

With conditions critical to main rotor flapping identified, a revised flapping design criteria was developed. This criteria is stated in the structural design terminology of limit and ultimate flapping magnitudes.

7.1 LIMIT FLAPPING CRITERIA

A limit flapping criteria is adequately defined in current design specifications (Reference 1.) This limit criteria applies for all operations within the recommended flight envelope and specifies:

- no contact with flapping stops except during stopping or starting the rotor
- airframe clearance of not less than 9 inches

No damage (other than tolerable fatigue damage) to the aircraft is permitted under normal flight operations within the operational limits specified by the manufacturer. Recommended flight envelopes, specifying weight, center of gravity, density altitude, rotor rpm, load factor, and airspeed limits, are supplied to the user. These limits are based on handling qualities, structural loading, and performance limits. In qualifying the helicopter, adequate flapping clearance will be demonstrated. However, it should be noted that, once in service, the aircraft may be flown outside the recommended limits due either to failures or to misuse by the user. When this occurs, limit flapping could be exceeded.

7.2 ULTIMATE FLAPPING CRITERIA

The ultimate flapping criteria would apply to all possible out-of-recommended flight envelope flight conditions and failure conditions that cannot be shown to be extremely remote. The proposed ultimate criteria require:

- no failure of primary structure due to flapping stop contact
- no contact of the rotor blade with the airframe

The ultimate envelope should encompass all probable out-of-recommended envelope conditions or failure conditions that can occur in service. Only conditions whose probability of occurrence is extremely remote would be excluded.

Defining the ultimate envelope requires determining the conditions that are to be considered and calculating loads due to excessive flapping.

7.2.1 Design Conditions

In determining out-of-envelope conditions that are not remote, suppositions of extreme loading conditions, such as excessive gross weight and out-of-cg limits, are likely. Limits, such as rpm, airspeed, and flight maneuvers, must be considered.

A pilot model must be used to establish the boundaries of flight conditions that are remotely possible that need be considered. A rational approach that includes possible control inputs, fuselage rates and attitudes, airspeeds, rotor rpm variations, and pilot training and awareness of the results of operation beyond the limits, is required. A possible approach to this design requirement would be to establish reasonable maximum values for these parameters and to apply a margin of safety on the design maneuver. The major difficulty here will be to establish a reasonable number of combinations of conditions that cover the more critical maneuvers.

7.2.2 Design Loads

Current design specifications require a rotor blade to airframe clearance of more than 9 inches under all flight conditions. For ultimate flapping, zero clearance would be a reasonable limit. To require that there be no damage to the airframe or blades due to in-flight contact would be too severe.

Once the limit conditions of no-contact-with-the-flapping-stops is exceeded, the loads and resultant blade-pylon-fuselage motions must be calculated. An existing BHT hybrid computer program was used to calculate examples of mast shear and moments due to flapping stop contact in hover for a teetering rotor helicopter. Blade, mast, and fuselage flexibility effects were included in this model. However, this model was not scaled for loads seen during flapping stop contact, and the magnitudes of the computed loads were not considered to be sufficiently accurate. Figure 29 illustrates the type of load spikes in the mast shear and bending moment due to flapping stop contact, and the significant increases in these loads as the blades attempt to flap beyond the stop.

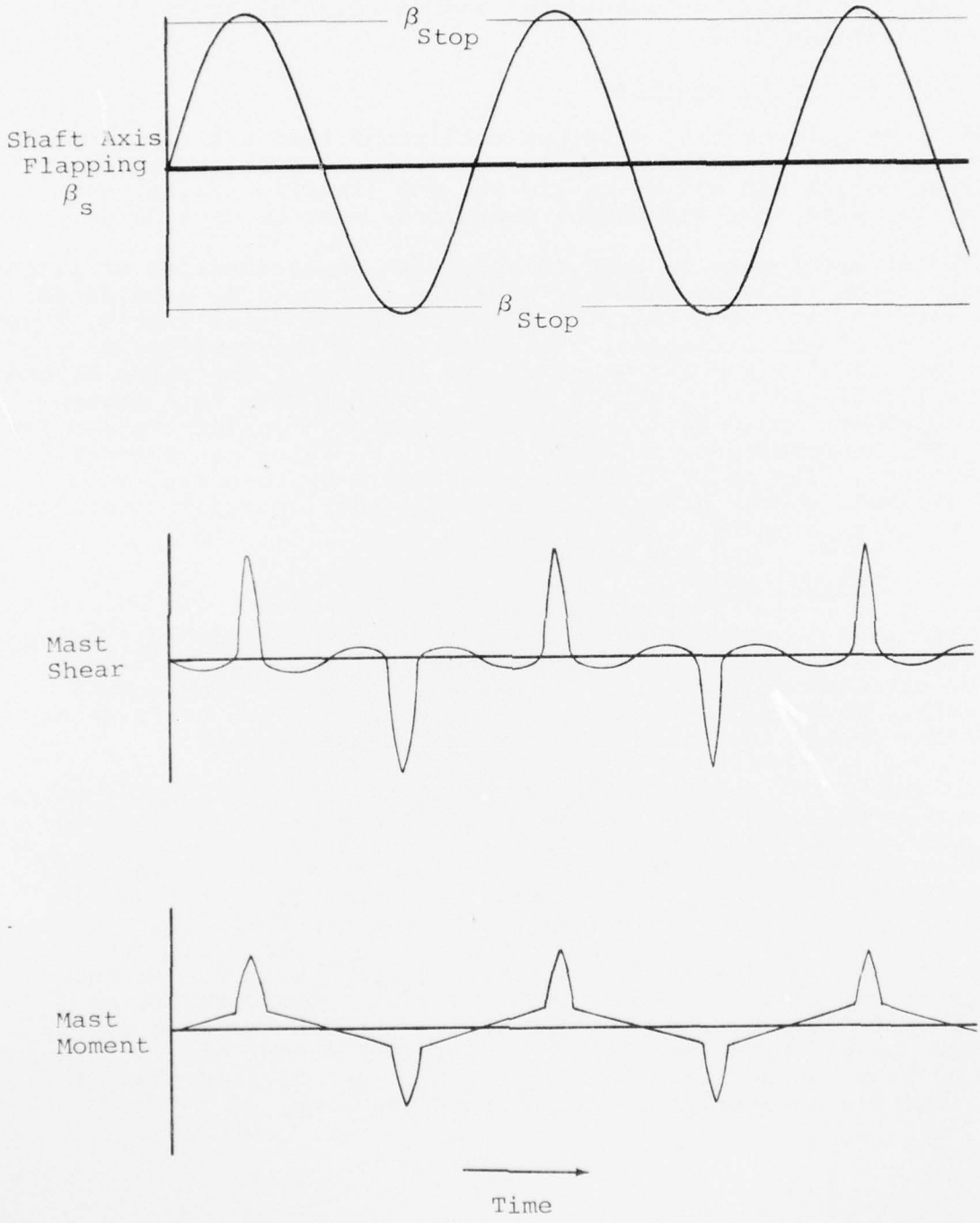

Figure 29. Sample mast shear and moment loads during flapping stop contact.

8. CONCLUSIONS AND RECOMMENDATIONS

8.1 CONCLUSIONS

This study did not reveal any unknown flapping characteristics. In all cases large flapping amplitudes could be explained by factors identified in the parametric study. Large flapping amplitudes could be expected when the simulated helicopters were operated under any of the following conditions:

- at center of gravity extremes
- under low- or negative-g conditions
- with large, abrupt control inputs
- in conditions involving significant retreating blade stall

The study indicates that if a helicopter is operated outside its recommended flight envelope, excessive flapping can occur.

The principle helicopter characteristics that influence flapping are:

- flapping restraint
- fuselage stability characteristics
- helicopter loading conditions

A design criteria for flapping that reflects the structural design concepts of limit and ultimate conditions is proposed. The limit flapping criteria are taken from the current specifications:

- no contact with flapping stops except during stopping or starting the rotor
- airframe clearance of not less than 9 inches

The limit criteria applies for all operations within the recommended flight envelope.

The ultimate flapping criteria would apply to all possible out-of-recommended flight envelope flight conditions and failure conditions that cannot be shown to be extremely remote. The proposed ultimate criteria require:

- no failure of primary structure due to flapping stop contact

- no contact of the rotor blade with the airframe

8.2 RECOMMENDATIONS

Based on the results of this study, the desirability of the following items to reduce or eliminate excessive flapping are considered:

Most conditions which cause excessive flapping result from rapidly developing phenomena such as blade stall, landing loads, or abrupt, large control inputs. Blade flapping increases rapidly from acceptable to excessive angles in only one or two rotor revolutions, leaving little, if any, reaction time for the pilot to correct the situation. Devices such as flapping indicators or g-level indicators could not be used effectively with the reaction time available. However, these devices may be useful by indicating to the pilot when he is operating under conditions where caution is needed to avoid rapid control inputs which may trigger excessive flapping.

Since large, abrupt control inputs are a primary source of excessive flapping conditions, the desirability of a control rate limiter is considered. Limitation of pilot inputs is not normally considered a desirable feature because it impacts on handling qualities. A trade-off between acceptable control input rates and degradation of the aircraft handling qualities must be made to evaluate the feasibility of such a limiter. Since an acceptable control input rate under one flight condition may be unacceptable under other flight conditions, any modification to the control system or the stability and control augmentation system must consider all possible flight conditions.

The pilot is the ultimate controller of conditions that generate excessive flapping. The danger of large, abrupt control inputs in flight conditions near retreating blade stall, or low g-levels, should be emphasized in training. Flight maneuvers which are acceptable when the aircraft is held within its operational envelopes may result in excessive flapping if any of those envelopes are exceeded. Improved training methods and use of placards emphasizing the need to remain within operational envelopes would be desirable.

8.3 RECOMMENDATIONS FOR FURTHER STUDY

The analytical methods for predicting rotor flapping in severe maneuvers should be validated. It is recommended that flapping be calculated for structural demonstration maneuvers and compared to the measured flapping. Modifications to existing methods may be required.

A methodology to predict loads due to inflight flapping stop contact should be developed and validated. Data to verify the analytical method could be obtained from aeroelastic model tests and from helicopter tie-down or whirl-tower tests.

More work is needed to fully develop the proposed ultimate flapping design criteria. A method of determining out-of-recommended flight envelope flight conditions should be established. One means of doing this would be to conduct a detailed study of several existing helicopters to establish such conditions for these helicopters. Extension of the results could lead to development of a general criteria for the other than extremely remote conditions.

Means of extending the recommended flight envelopes of existing helicopters, where the flight envelope is restricted by allowable flapping, should be investigated.

AD-A034 459 BELL HELICOPTER TEXTRON FORT WORTH TEX F/G 1/3
ROTOR BLADE FLAPPING CRITERIA INVESTIGATION.(U)
DEC 76 L W DOOLEY DAAJ02-75-C-0030
UNCLASSIFIED 699-099-021 USAAMRDL-TR-76-33 NL

2 OF 2
AD A034459

END

DATE
FILMED
2 -77

LITERATURE CITED

1. Anon., MILITARY SPECIFICATION - STRUCTURAL DESIGN REQUIREMENTS - HELICOPTERS, MIL-S-8698 (ASG), Naval Publications and Forms Center, Washington, D.C., February 1958.

2. Anon., STRUCTURAL DESIGN REQUIREMENTS (HELICOPTERS), AR-56, Naval Air Systems Command, Department of the Navy, Washington, D.C., February 1970.

3. Anon., ENGINEERING DESIGN HANDBOOK, HELICOPTER ENGINEERING, PART ONE: PRELIMINARY DESIGN AMCP 706-201, U.S. Army Materiel Command, Alexandria, Virginia, August 1974.

4. Anon., GENERAL SPECIFICATION FOR DESIGN AND CONSTRUCTION OF AIRCRAFT WEAPON SYSTEMS, VOLUME II - ROTARY WING AIRCRAFT, SD-24K, Naval Air Systems Command, Department of the Navy, Washington, D.C., December 1971.

5. Anon., CIVIL AIR REGULATIONS - PART 6 - ROTORCRAFT AIRWORTHINESS: NORMAL CATEGORY, Federal Aviation Administration, Department of Transportation, Wahington, D.C., December 1966.

6. Anon., FEDERAL AVIATION REGULATIONS, PART 27: AIRWORTHINESS STANDARDS: NORMAL CATEGORY ROTORCRAFT, Federal Aviation Administration, Department of Transportation, Washington, D.C., August 1974.

7. Davis, J. M., et al, ROTORCRAFT FLIGHT SIMULATION WITH AEROELASTIC ROTOR AND IMPROVED AERODYNAMIC REPRESENTATION, USAAMRDL Technical Report 74-10A, B, C, Eustis Directorate, U.S. Army Air Mobility Research and Development Laboratory, Fort Eustis, VA, June 1974, AD 782854, 782756, and 782841.

8. Brown, E. L., and Schmidt, P. S., THE EFFECT OF HELICOPTER PITCHING VELOCITY ON ROTOR LIFT CAPABILITY, Journal of the American Helicopter Society, Vol. 8, No. 4, October 1963.

9. Amer, K. B., THEORY OF HELICOPTER DAMPING IN PITCH OR ROLL AND A COMPARISON WITH FLIGHT MEASUREMENTS, Technical Note 2136, NACA, October 1950.

10. Springer, R. H., and Berger, D., CATEGORY II PERFORMANCE TEST OF THE UH-1J HELICOPTER, VOLUME II, Technical Report No. 72-17, U.S. Air Force Flight Test Center, Edwards AFB, Calif., May 1972.

11. Harris, F. D., ARTICULATED ROTOR BLADE FLAPPING MOTION AT LOW ADVANCE RATIO, Journal of the American Helicopter Society, Vol. 17, No. 1, January 1972, pp. 41-48.

LITERATURE CITED - Concluded

12. Bennett, R. L., DIGITAL COMPUTER PROGRAM DF1758: FULLY COUPLED NATURAL FREQUENCIES AND MODE SHAPES OF A HELICOPTER ROTOR BLADE, Report No. 299-099-724, Bell Helicopter Textron, Fort Worth, Texas, March 1975.

13. Harvey, K. W., Blankenship, B. L., and Drees, J. M., ANALYTICAL STUDY OF HELICOPTER GUST RESPONSE AT HIGH FORWARD SPEEDS, USAAVLABS Technical Report 69-1, U.S. Army Aviation Materiel Laboratories, Fort Eustis, VA, September 1969, AD 862594.

14. Damon, A., Stoudt, H. W., and McFarland, R. A., THE HUMAN BODY IN EQUIPMENT DESIGN, Cambridge, Mass., Harvard University Press, 1966.

LIST OF SYMBOLS

a	lift curve slope, 1/rad
a_{o_s}	coning angle, shaft axis, rad
a_{1_s}	longitudinal flapping, shaft axis, rad
A_o	collective pitch angle, rad
A_1	lateral cyclic pitch angle, rad
b_{1_s}	lateral flapping, shaft axis, rad
B_1	longitudinal cyclic pitch angle, rad
C	chord, ft.
c_{1_s}	maximum flapping angle $= \sqrt{a_{1_s}^2 + b_{1_s}^2}$, rad
C_T	rotor thrust coefficient $= T/\rho(\Omega R)^2 b\ c\ R$
e	flapping hinge offset from shaft, ft
GW	helicopter gross weight, lb
h	distance from rotor hub to helicopter center of gravity, ft
I_b	flapping inertia of rotor blade, slug-ft^2
K_H	flapping restraint spring constant, ft-lb/rad
ℓ_β	fuselage rolling moment due to sideslip, ft-lb/deg
p	helicopter roll rate, rad/sec^2
q	helicopter pitch rate, rad/sec^2
R	rotor radius, ft
t	time, sec
t_o	control input time, sec
β	sideslip angle, deg

LIST OF SYMBOLS - Continued

β_{K_H}	flapping of rotor with hub restraint, rad
$\beta_{K_H=0}$	flapping of rotor with no hub restraint, rad
β_s	rotor tip path plane angle, shaft axis, rad
γ	Lock number = ρ a c R^4/I_b
θ	blade pitch, rad
μ	rotor advance ratio
ρ	air density, slugs/ft^3
σ	rotor solidity
τ	first order system time constant, sec
ϕ	phase angle of maximum flapping, rad
ψ	azimuth, rad
Ω	rotor rotational speed, rad/sec